



UNIVERSITEIT•STELLENBOSCH•UNIVERSITY
jou kennisvenoot • your knowledge partner

Design of a Pump-As-Turbine Microhydro System for an Abalone Farm

BH Teuteberg

March, 2010



Departement Meganiese en Megatroniese Ingenieurswese
Department of Mechanical and Mechatronic Engineering



Design of a Pump-As-Turbine Microhydro System for an Abalone Farm

Final Report for Mechanical Project 878

BH Teuteberg

Supervisor: Prof W van Niekerk

Department of Mechanical and Mechatronic Engineering
Stellenbosch University

March, 2010

I, Bernhard Hein Teuteberg, declare that I have not accepted outside help regarding the project, either from fellow students or from anybody else.

Bernhard Hein Teuteberg

Prof. W. Van Niekerk

ABSTRACT

This document details the design process of a 97 kW microhydro system for Roman Bay Sea Farm in Gansbaai in the Western Cape Province of South Africa. It contains a literature study of microhydro power, with a focus on the use of Pump-as-Turbine technology and direct-drive systems. The literature study leads to several possible concepts for the project, which are then evaluated and the most suitable design is found to be a reverse running pump that powers a different pump through a direct drive system. Experimental data from KSB is used to test the accuracy of various correlations that can be used to generate turbine-mode operation curves from pump curves. The final design parameters for the complete system are then determined, and presented along with a cost-benefit analysis.

OPSOMMING

Hierdie verslag dokumenteer die ontwerpsproses van 'n 97 kW mikro hidro stelsel vir Roman Bay Sea Farm in Gansbaai in die Wes Kaap van Suid Afrika. Dit bevat 'n literatuurstudie van mikro hidro krag, met 'n fokus op Pomp-as-Turbine en direk-gekoppelde stelsels. Die literatuurstudie lei tot 'n aantal moontlike konsepte vir die projek wat dan evalueer word sodat die mees gepasde ontwerp gekies kan word. Dit word gevind dat 'n pomp wat verkeerd om hardloop en 'n ander pomp direk van krag voorsien die mees gepasde ontwerp is. Eksperimentele data van KSB word gebruik om die akkuraatheid van verskeie korrelasies te toets wat gebruik kan word om turbine-mode gedrag van pomp kurwes te bepaal. Die finale parameters van die hele stelsel word dan bepaal en word dan saam met 'n koste-analise aangebied.

CONTENTS

Page

Abstract.....	ii
Opsomming.....	ii
List of Figures	iv
List of Tables	v
List of Symbols	vi
List of Subscripts and Acronyms	vi
1. Introduction.....	1
2. Literature study	3
2.1 Microhydro systems	3
2.2 Water filtering	3
2.3 Penstock	4
2.4 Turbine.....	5
2.4.1 Typical turbines.....	5
2.4.2 Pump-as-Turbine (PAT).....	7
2.5 Power.....	13
2.5.1 Generator.....	13
2.5.2 Linked PAT and pump	15
3. Computer simulation.....	18
4. Current setup and future expansion at Roman Bay.....	23
4.1 Pump models and average flow rate	23
4.2 Outflow	24
4.3 Future expansion	24
4.4 Proposed site to investigate	25
5. Concept evaluation	26
6. System design.....	34
6.1 Turbine selection	34
6.2 Driven pump section	37
6.3 Specification of remaining components.....	37
7. Project costs	41
8. Summary.....	44
9. References.....	45
Appendix A: Fluid property determination	48
Appendix B: Turbine cost prediction formulas.....	49
Appendix C: BUTU method for predicting PAT performance from pump performance data.....	50
Appendix D: Performance factor diagrams from the method of Chapallaz et al. (1992)	51
Appendix F: Pump and Turbine mode curves of various KSB centrifugal pumps .	54

LIST OF FIGURES

Figure 1: Slanted box cleaning system (Cunningham & Woofenden, 2007) and Leaf mulcher (Aronson, 2008)	4
Figure 2: Rough guide to turbine type operating ranges (adapted from Chapallaz et al. 1992)	5
Figure 3: Types of impulse turbines (Western North Carolina Renewable Energy Initiative, 2007)	6
Figure 4: Low Head turbines	6
Figure 5: Turbine Operation vs. Pump Operation Characteristic curves (Baumgarten & Guder, 2005)	7
Figure 6: Choice of pumps for PAT applications (adapted from Chapallaz et al, 1992)	8
Figure 7: "C-2C" Three phase induction motor connection	14
Figure 8: Linked shaft PAT/pump system in Java, Indonesia (Baumgarten & Guder, 2005)	16
Figure 9: Assembled linked shaft PAT/pump system Indonesia (Baumgarten & Guder, 2005)	17
Figure 10: Inlet loss coefficients	21
Figure 11: Screenshot of the simulation program	22
Figure 12: Map of Roman Bay showing important areas	23
Figure 13: Outlet water flow	24
Figure 14: Outlet water channel	25
Figure 15: Overview of design decisions to be made	28
Figure 16: The four different concepts considered for this project	29
Figure 17: Concept design of system	34
Figure 18: Correlation results versus experimental results	35
Figure 19: Percentage error in correlation flow and head	36
Figure 20: Reservoir Diagram	38
Figure 21: Schematic of final system	39
Figure 22: Setup inside pump house	40
Figure 23: Eskom electricity tariff periods (Eskom, 2009)	42
Figure 24: Performance factors, head versus flow	51
Figure 25: Performance factors, power versus flow	51
Figure 26: Factors for calculating head away from BEP	52
Figure 27: Factors for calculating power away from BEP	53
Figure 28: Omega 350-510A in turbine mode	54
Figure 29: Omega 350-510A in pump mode	55
Figure 30: Pump curve of KSB LCC-M 200-610 pump	56

LIST OF TABLES

Table 1: Differences between turbines and PAT	9
Table 2: Differences between generators and direct drive systems.....	15
Table 3: Values of pipe roughness for various materials.....	20
Table 4: Head loss coefficient for various pipe segments	21
Table 5: Pump flow rates	23
Table 6: Client and engineering specifications	26
Table 7: Advantages and disadvantages of the two direct-drive system pump choices	30
Table 8: Cost prediction results	30
Table 9: Estimates of turbine costs for various systems	31
Table 10: Cost per installed kilowatt of electro-mechanical equipment	32
Table 11: Total costs of each concept (ex VAT).....	33
Table 12: Total cost per kilowatt-hour for each concept	33
Table 13: Rough estimates of preliminary costs for complete system	41
Table 14: Roman Bay Sea Farm electricity prices (according to Angelo Bucchianeri from Roman Bay Sea Farm)	42

LIST OF SYMBOLS

C	Conversion factors
D, d	Pipe diameter
e	Pipe roughness factor
f	Friction factor
g	Gravitational acceleration
H	Head
h	Ratio of pump head to turbine mode head
k_i	Head loss coefficient
L	Length
N	Specific speed
P	Power
p	Pressure
Q	Flow rate
Re	Reynolds number
S	Salinity
T	Temperature
t	Thickness
v	Fluid velocity
α	Dimensionless specific speed
γ	Dimensionless parameter
η	Turbine efficiency
ν	Kinematic viscosity
ρ	Density
σ	Stress

LIST OF SUBSCRIPTS AND ACRONYMS

Bep, r	Best Efficiency Point
CFD	Computational Fluid Dynamics
GPS	Global Positioning System
GUI	Graphical User Interface
IPP	Independent Power Producer
max	Maximum
NERSA	National Energy Regulator of South Africa
NMHP	Nepal Micro Hydro Power
p	Pump mode
PAT	Pump as Turbine

REFIT

t

VAT

Renewable Energy Feed-in Tariff

Turbine mode

Value Added Tax

1. INTRODUCTION

Roman Bay Sea Farm is an abalone farm on the south coast of South Africa which uses a large amount of seawater in the various growing cycles of the farm. The abalone first go through breeding, larvae, settlement and weaning stages in the hatchery where a small amount of water is cycled, and then they are moved to the growing blocks where most of the water is used. The water is pumped up from the ocean to holding tanks on the farm where it is stored. It is then gravity-fed to the various processes of the farm and after the water has passed through the farm it returns to the ocean by means of a single pipe.

The rising electricity cost in South Africa has caused Roman Bay Sea Farm to start investigating means of reducing their energy consumption. This proposal stems from a renewable energy study done by the Centre for Renewable and Sustainable Energy Studies at Stellenbosch University (Meyer & Van Niekerk, 2008) where it was found that the returning flow of seawater could generate a theoretical maximum of 127 kW of power. By harnessing this power Roman Bay Sea Farm can both reduce their electricity consumption and provide a small backup power supply in case of power interruption.

Meyer and Van Niekerk (2008) proposed using a pump-as-turbine (PAT) system to generate the power as local manufacturers of turbines are very limited. Other reasons to use a PAT system include that they are typically cheaper and easier to install, maintain and operate (Smit, 2005). A mechanical connection between the PAT system and one of the pumps was also investigated. The purpose of this would be to reduce losses that would be incurred by the conversion from mechanical power to electricity and back, thereby increasing the overall efficiency of the system.

This project studied the recovery of energy from the returning flow of seawater from the farm. This energy can then be used to power the existing pumps or other energy needs of the farm. The energy will be recovered by a micro hydro system and the possibility of using pump-as-turbine technology will be investigated, along with the use of a mechanical connection between the turbine and the current pumps installed at Roman Bay. The main goals are thus as follows:

- a. To recover energy from the returning flow of seawater that can be used to reduce the overall energy consumption of Roman Bay Sea Farm.

Calculate the total amount of energy that can be recovered from seawater flow. Investigate the advantages and disadvantages of both Pump-as-Turbine technology and a mechanical connection between the turbine and currently installed pumps.

- b. To complete an engineering design for the proposed system.

Determine the engineering design parameters of the selected configuration. The final report should contain a complete specification of the required equipment and the costs thereof. The total cost of the project must then be weighed against the electricity savings in order to determine the financial viability of the project.

In this report the design of a microhydro system for Roman Bay Sea Farm is documented. It contains a literature study on traditional microhydro systems and then presents a case for Pump-as-Turbine technology as a cost-effective alternative to traditional turbines. Several experimentally determined correlations are shown that can be used to predict turbine mode performance from pump curves. To assist with the design process a user-friendly computer simulation program is developed that can analyse hydro potential for various sites. This follows into a concept design section where several concepts are discussed and evaluated until the outline of the final system is determined. The final concept then undergoes a detail design process where the complete engineering specifications of the system are determined and finally a summary of the results are given.

2. LITERATURE STUDY

2.1 Microhydro systems

“Micro” hydro systems typically refer to hydro power systems that have a power output of between 100 kW and 500 kW (Pigaht and van der Plas, 2009). The systems are mostly designed to provide power for household use and small communities. The major advantage of this system when compared to other renewable energy technologies is that, if enough water is available, it can provide a constant and/or predictable power supply, whereas other technologies (specifically wind and solar power) provide intermittent or unpredictable energy.

A complete microhydro system consists of the following major components, which are discussed in this section.

- Water filtering mechanism
- Penstock with valves
- Turbine
- Power-converting device (Generator or direct-drive)

2.2 Water filtering

A major aspect of system design that often is not considered is the removal of solid bodies from the water before it enters the turbine. If no such system is installed the turbine could suffer damage from sticks and stones, as well as reduced performance from leaves that get stuck on the blades. As this can never be totally removed the turbine will probably require cleaning at some stage for this design.

There are several technologies available in order to stop these solid bodies from damaging the turbine or reducing its performance. A slanted box may be used in order to remove any surface material and then the outlet pipe may be situated higher than the bottom of the box so that any rocks are also removed, according to Cunningham & Woofenden (2007). This method requires that the box be cleaned at certain times as the debris will build up at the bottom. The slanted box can be seen in Figure 1.



Figure 1: Slanted box cleaning system (Cunningham & Woofenden, 2007) and Leaf mulcher (Aronson, 2008)

Another method would be to make use of a leaf mulcher, which according to Aronson (2008) is a piece of plastic with its end shaped to mirror the ends of the turbine blades. As the blades spin the leaves are moved to the outside due to centrifugal force where they are removed by the mulcher. This can be seen in Figure 1 as well.

2.3 Penstock

Following on the intake a length of pipeline is needed to direct the water to the turbine. Depending on the pressure in the pipeline it may be made of PVC or one of many other alternatives. The material should be appropriate to the application, which may in some cases be seawater. The pipe should also be strong enough to withstand the water pressure caused by the change in head.

The diameter of the pipe should be chosen so as to minimize friction losses without inflating the cost. In Smit (2005) this is done by analyzing the friction losses at certain diameters in order to obtain a graph of the results, from which an appropriate diameter can be chosen.

The pipeline is sometimes buried in order to protect the water inside from freezing or to protect the pipe from damage, either by UV rays, or by animals or other mechanical damage. While freezing is not an issue in most of South Africa, it may be desirable to bury the pipeline to protect it from damage.

2.4 Turbine

2.4.1 Typical turbines

The turbine is situated after the pipeline and can be either classified as low or high head. The term “head” refers to the elevation difference between the inlet and outlet of the system. Different turbines are used for each situation, with high head systems normally using turbines such as Pelton wheels or Turgo runners, according to Western North Carolina Renewable Energy Initiative (2007). Low-head systems typically use Francis, Kaplan or Crossflow turbines to turn the generator. A rough guide to turbine choice is given in Figure 2.

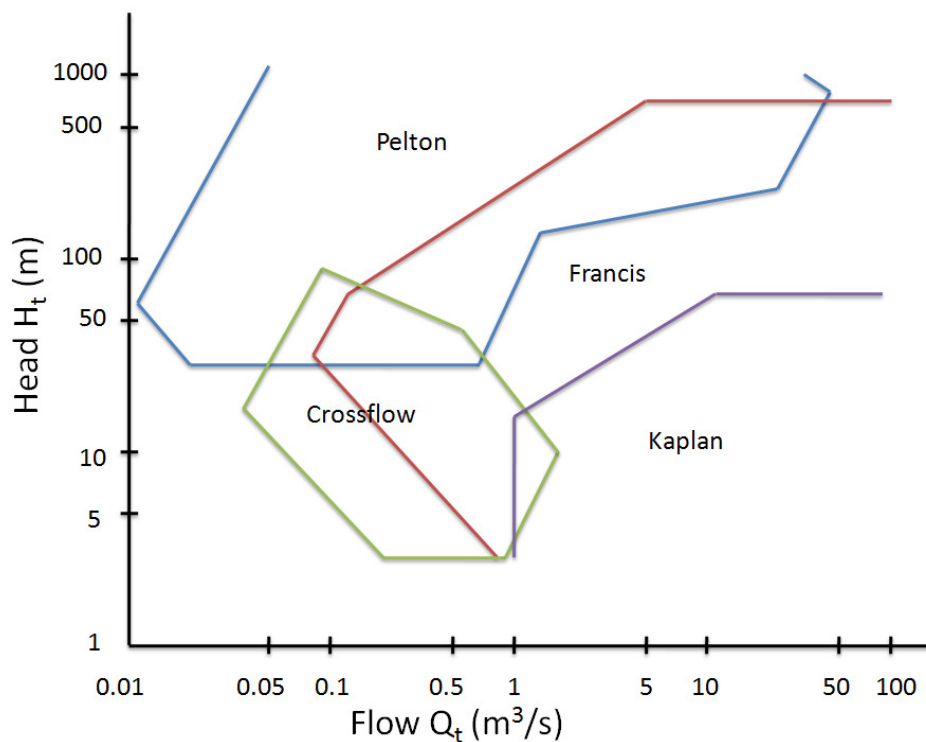


Figure 2: Rough guide to turbine type operating ranges (adapted from Chapallaz et al. 1992)

The high-head turbines mostly use the impulse method, where the water is routed to nozzles which turn a wheel or runner. Two of these turbines are shown in Figure 3.

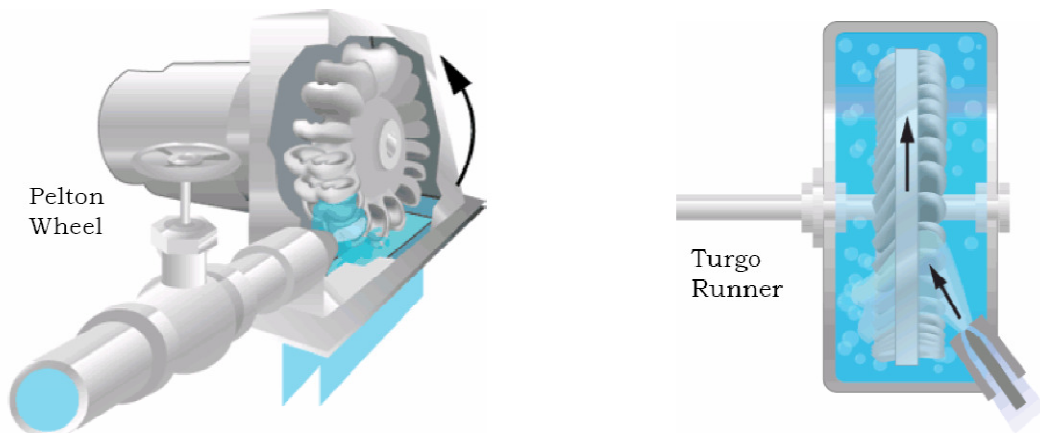


Figure 3: Types of impulse turbines (Western North Carolina Renewable Energy Initiative, 2007)

Low-head turbines are usually reaction type turbines that use a large flow of water over a small head to generate power. The turbines are sometimes located directly in the flow of a river, which is where the “run-of-the-river” term comes from. As the low head usually equates into a slower flow velocity the turbines also usually turn slower than the high head turbines, but produce greater torque.

Schematic drawings of two of these turbines are given in Figure 4.

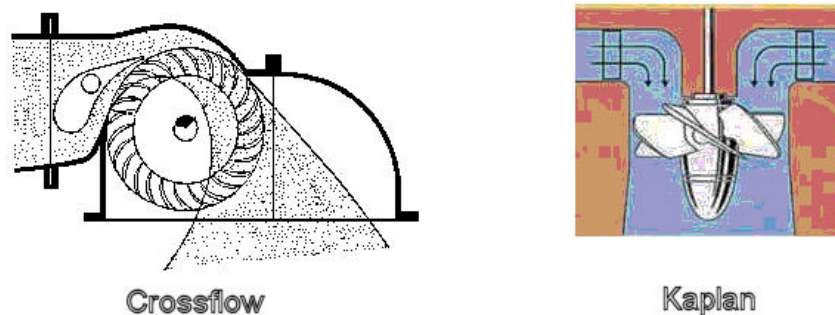


Figure 4: Low Head turbines

Ogayar and Vidal (2009) provide a set of formulas that predict the cost per kilowatt of the electro-mechanical equipment (turbine, generator and regulator) for the most common turbines, namely Pelton, Francis, Kaplan and semi-Kaplan, for a power range below 2 MW. The exact equations are given in Appendix B, and are of the basic format given in equation 4.1.

$$COST = aP^{b-1}H^c \quad (2.1)$$

It can be seen that the cost is a function of the net head (H) and the power (P), with the coefficients a , b and c dependant on the location, turbine and time at which the analysis is done. Using data from real installations worldwide, the coefficients were determined for each of the types of turbine. The accuracy of the formulas was found to be within 20% for most cases.

2.4.2 Pump-as-Turbine (PAT)

In recent times however pump-as-turbine (PAT) systems have become popular. In such a system a pump is operated in reverse so that it functions as a turbine. This is especially popular in areas where the availability of turbines is limited as pumps are typically easier to get hold of.

Derakhshan & Nourbakhsh (2008) state that pumps are relatively simple and easy to maintain. They also have a competitive maximum efficiency when compared to conventional turbines. Baumgarten & Guder (2005) propose that the major benefit is that mass production of pumps means that they are comparatively much more cost-effective than conventional turbines.

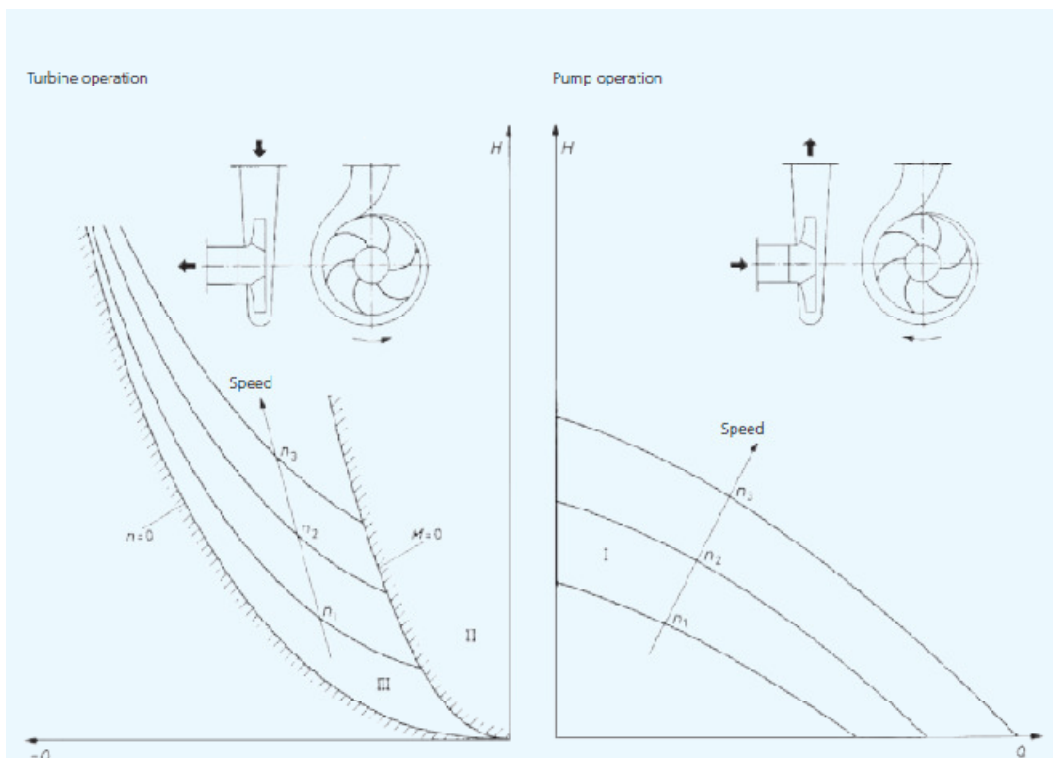


Figure 5: Turbine Operation vs. Pump Operation Characteristic curves (Baumgarten & Guder, 2005)

The preceding Figure 5 shows basic characteristic curves for a pump operating in pump and turbine mode. The line “M=0” is the zero-load curve which is when no torque is imparted to the shaft and the “n = 0” line is the standstill curve which is when the pump is subjected to forced flow without the shaft turning. The centrifugal pump operates as a turbine in between these two lines.

As there are many different types of pumps that can be used as a turbine, Chapallaz et al. (1992) gives the rough guide in Figure 6 to aid the choice. Multistage pumps are only typically used in cases where the head is very high, and when the flow rate is high either multistage pumps or a system of single flow pumps in parallel is used.

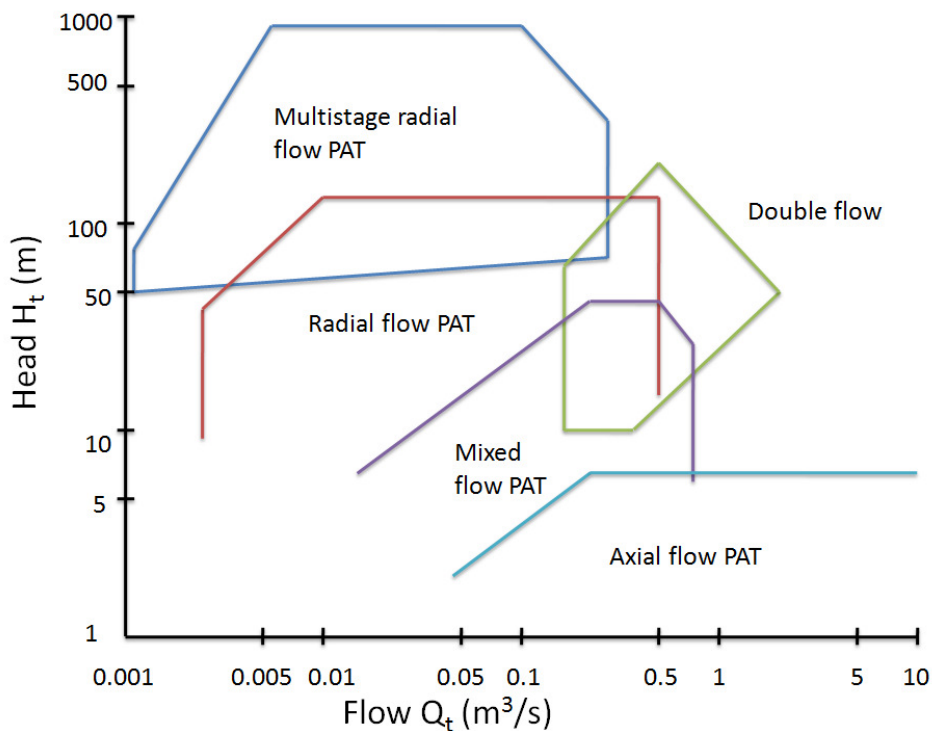


Figure 6: Choice of pumps for PAT applications (adapted from Chapallaz et al, 1992)

According to Williams (1996) the main disadvantage of PAT systems is that the characteristics curves in turbine mode are not usually supplied with the pump. This makes it hard to choose the correct pump for each application and so several methods have been developed in order to predict turbine mode characteristics.

Table 1 shows some of the major differences between PAT systems and conventional turbines.

Table 1: Differences between turbines and PAT

	Turbine	PAT
Advantages	Well-documented	Cost-efficient
	Best efficiency	Widely available locally and abroad
	Variable Guide vanes for varying flow	Simple design and easy maintenance
Disadvantages	Expensive	Difficult to find correct turbine operation curves
	Very few local suppliers	Lower efficiency
	Complex design may require expert maintenance	No variable guide vanes for varying flow
		Not as well-documented as turbines

Nepal Micro Hydro Power (2005) predicted direct factors of 1.38 for the head and 1.25 for the flow rate of the any pump operating as a turbine. However, when Smit (2005) did experiments on a PAT system the experimental data showed a factor of 2 for the head and 1.65 for the flow rate. This shows that while this method is simple to use, the factors vary considerably depending on pump make and even model. As such the factors should only be used when experimental data can be obtained from the manufacturer, and then only for pumps that are very similar in construction.

Another simple method is proposed by Sharma (1985) where the flow rate and head at best efficiency point for the pump (Q_{bep} and H_{bep}) is related to the turbine flow rate and head (Q_t and H_t) by the maximum efficiency (η_{max}) of the pump. The following equations describe the relationship.

$$Q_t = \frac{Q_{bep}}{\eta_{max}^{0.8}} \quad (2.2)$$

$$H_t = \frac{H_{bep}}{\eta_{max}^{1.2}} \quad (2.3)$$

The method of Stepanoff (1957), which is based on theoretical considerations, calculates the performance of a pump operated as a turbine using the following two relations.

$$H_t = \frac{H_{bep}}{\eta_{max}} \quad (2.3)$$

$$Q_t = \frac{Q_{bep}}{\sqrt{\eta_{max}}} \quad (2.4)$$

McClaskey and Lundqvist (1976) use equation 2.5 for Q_t .

$$Q_t = \frac{Q_{bep}}{\eta_{max}} \quad (2.5)$$

An empirical method, based on curve fitting of experimental data, is presented in the BUTU method (Chapallaz, et al., 1992). The method predicts turbine performance at both Best Efficiency Point (BEP) and values away from this point. This is very valuable as a selected PAT will typically not operate at exactly its BEP but somewhere close to it. The formulas are given in Appendix C, as they are rather complicated and thus more suited to computer implementation than calculation by hand. The errors incurred in this method are reported to be around 10% and more.

While the previous methods all determined turbine mode performance from pump curves, Derakhshan & Nourbakhsh (2007) propose another method to choose a pump for a PAT system based on the required turbine mode characteristics. The method is based on relations found in the experimental testing of several centrifugal pumps in reverse.

The pump specific speed in its operating point, N_{rp} can be calculated by using equation 2.6.

$$N_{rp} = 0.3705N_{rt} + 5.083 \quad (2.6)$$

where N_{rt} and N_{rp} are the turbine and pump specific speeds in their rated points, respectively.

The dimensionless specific speed of the pump is calculated in equation 2.7.

$$\alpha_p = \frac{N_{rp}}{g^{0.75}} \quad (2.7)$$

in order to find dimensionless parameter γ in equation 2.8.

$$\gamma = 0.0233\alpha_p + 0.6464 \quad (2.8)$$

Now γ is used so that h (the ratio of pump head to turbine mode head) can be determined using equation 2.9.

$$\gamma = \frac{(h^{-0.5})N_t}{N_p} \quad (2.9)$$

H_{pr} is the head of the pump at the rated point. It is calculated by equation 2.10 where H_{tr} is the available head for the PAT.

$$H_{pr} = \frac{H_{tr}}{h} \quad (2.10)$$

Q_{pr} can be obtained using N_{rp} , choosing N_p from a list of available pumps and knowing H_{pr} .

The proper PAT can be easily selected when H_{pr} , Q_{pr} and N_p are known. These define the design point at which a pump should work in order to function at its best efficiency point as a turbine. It is also noted that this procedure is only valid for turbines with $N_{st} < 150$.

They further report that a PAT operates at a higher head and flow rate than in pump mode at the same rotational speed and that the efficiencies remain almost the same. The results from the correlation proved to coincide with the experimental data used in Derakhshan & Nourbakhsh (2007) but it is also stated that the method remains a correlation and may thus prove inaccurate in other cases. As the study was limited to four different pumps the accuracy over a

larger range of pumps can also be questioned. The method was however found to be more accurate than the method of Sharma (1985), as well as other methods described by Stepanoff (1957) and Alatorre-Frenk (1994).

The final method that will be described here is found in Chapallaz et al. (1992). This method again uses experimental data to determine empirical correlations, but in this case over 80 different pumps were used. The method allows the user to select candidate pumps, and following these initial choices, it continues as follows in order to select the best possible pump.

Determine the rated pump head, flow and maximum efficiency and if the pump has multiple stages or entries, convert the head and flow into single-stage equivalents. These values can typically be found on the data sheets of most pump manufacturers.

Calculate the specific speed of the pump using equation 2.11

$$N_p = n_p \frac{\sqrt{Q_{pr}}}{H_{pr}^{\frac{3}{4}}} \quad (2.11)$$

The conversion factors C_H and C_Q can be read from the diagrams in Figure 24 and Figure 25 in Appendix D using the maximum efficiency of the pump. Now use the following scatter factors to determine the performance range of the PAT.

$$\begin{aligned} C_{Hmax} &= 1.1C_H \\ C_{Hmin} &= 0.9C_H \\ C_{Qmax} &= 1.075C_Q \\ C_{Qmin} &= 0.925C_Q \end{aligned} \quad (2.12)$$

Now it is simple to determine the maximum and minimum turbine design head and flow at the rated pump speed and then convert this to the nominal turbine speed by substituting the appropriate factors in equation 2.13.

$$H_{tmax}(nt) = \frac{C_{Hmax}H_{rp}n_t}{n_p} \quad (2.13)$$

The maximum efficiency of the pump in turbine mode is given by equation 2.14

$$\eta_{tmax} = \eta_{pmax} - 0.03 \quad (2.14)$$

And now the minimum and maximum power output can be obtained using the head, flow rate and efficiency.

In order to determine the shape of the curve away from the BEP, the diagrams in Figure 26 and Figure 27 in Appendix D are used. These diagrams give the head and power as function of the flow rate for various specific speeds. The resulting curves can now provide a good estimate of the performance of the pump in turbine operating mode.

While it is clear that there are many correlations available, the accuracy of all of them can be questioned under certain conditions and as such these methods are mostly useful as a rough guide to aid design decisions. It may be possible to gain sufficient accuracy using Computational Fluid Dynamics (CFD) software, as found in Rawal & Kshirsagar (2007) and Derakhshan & Nourbakhsh (2008), but this may not be a viable option in all cases as it is quite an intensive and expensive process and also differs for each pump.

Fortunately there are certain pump manufacturers that test their pumps in turbine mode and can thus provide very accurate experimental data. This makes the design process much simpler, but as stated by Chapallaz et al. (1992) it does increase the cost of the turbine as the manufacturer has to conduct all the tests. In many cases this can result in exactly the same pump having two different prices, one for turbine mode and one for normal operating mode.

2.5 Power

2.5.1 Generator

Typically in microhydro systems the torque from the output shaft of the PAT is converted into electricity by use of a generator. This provides great flexibility for the use of the power as the electricity is easy to transport and use for multiple devices at the same time.

In converting the energy from the shaft into electricity some energy is lost. As the power from the turbine may be used to drive a pump, there will again be losses when the electricity is used in the pump motor. Kaya et al. (2008) report that motor efficiencies can range between 70% and 96% and higher efficiency motors normally cost 15-25% more than standard motors. Generator performance is comparable to motor performance and thus the range of typical total efficiencies for just the electrical sub-system would be between 50% and 92%. The efficiency of the motor is also relative to the load as motors running at partial load will be less efficient. It is thus crucial to choose the correct size for the motor and therefore also the generator.

Williams (1996) reports that synchronous generators were used previously but induction motors proved to be more suited to the application. They are more robust because of the method of construction which uses cast bars instead of windings on the rotating part. Most pump units are supplied with three-phase induction motors. This can be used to provide a single phase supply at up to 80% of the motor rating by using the so-called "C-2C" connection shown in Figure 7.

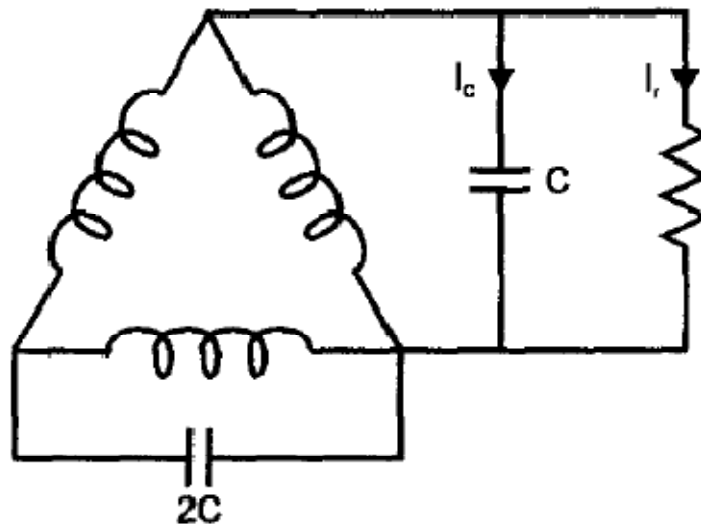


Figure 7: "C-2C" Three phase induction motor connection

As it is very difficult to operate the generator at constant load a controller is necessary to regulate the output voltage. Some of the commercially available units also offer good frequency regulation according to Williams (1996). The regulator functions by using a dump load where excess electricity can be sent when it is not being used. This normally takes the form of a resistance heater that heats either air or water.

2.5.2 Linked PAT and pump

The losses experienced in the generation and use of electricity may be avoided by connecting the shafts of the PAT and the pump. This means that most of the power generated in the PAT will reach the pump, with small losses experienced in possible clutches and gearboxes. However, a major negative aspect of this solution is that the location of the PAT system becomes more constrained as it needs to be situated next to the pump it would power.

This solution should be more efficient than a generator when powering a single constant load such as a pump which runs all the time. As soon as multiple or variable loads are to be powered by the PAT system a generator may prove to be a simpler and more effective solution. Table 2 summarizes the differences between generators and direct-drive systems.

Table 2: Differences between generators and direct drive systems

	Generator	Direct Drive Pump
Advantages	Produces electricity which can be used in various areas	Much higher total efficiency
	Can be purchased as a commercial package with the turbine/PAT	Simpler design, requires fewer components
	The reliability of the turbine/PAT will not affect the flow of water	Cheaper, if existing pumps can be driven
Disadvantages	Energy is lost in the generator	Pump has to run at same rotational speed as turbine/PAT or gearbox is required
	Requires a complex electrical regulating system with a dump load	Operation of system is dependent on reliability of both turbine/PAT and the pump.
	More expensive	The PAT/turbine has to be situated next to the pump

Baumgarten & Guder (2005) report on the use of such a linked PAT/pump system in Java, Indonesia. The island has a vast subterranean system of caves that has plentiful water supply, but lack of surface runoff during the dry season threatens the water supply of the island. The goal of the project is to use the potential energy in the flow of an underground river to pump water up to a storage tank on the surface from where it can be used (Figure 8). As the PAT's would be situated some 100 m below the ground and thus not tied into the grid, it was

decided to use the output shafts from the PAT's to directly power the pumps that send the water to the upper storage tank.

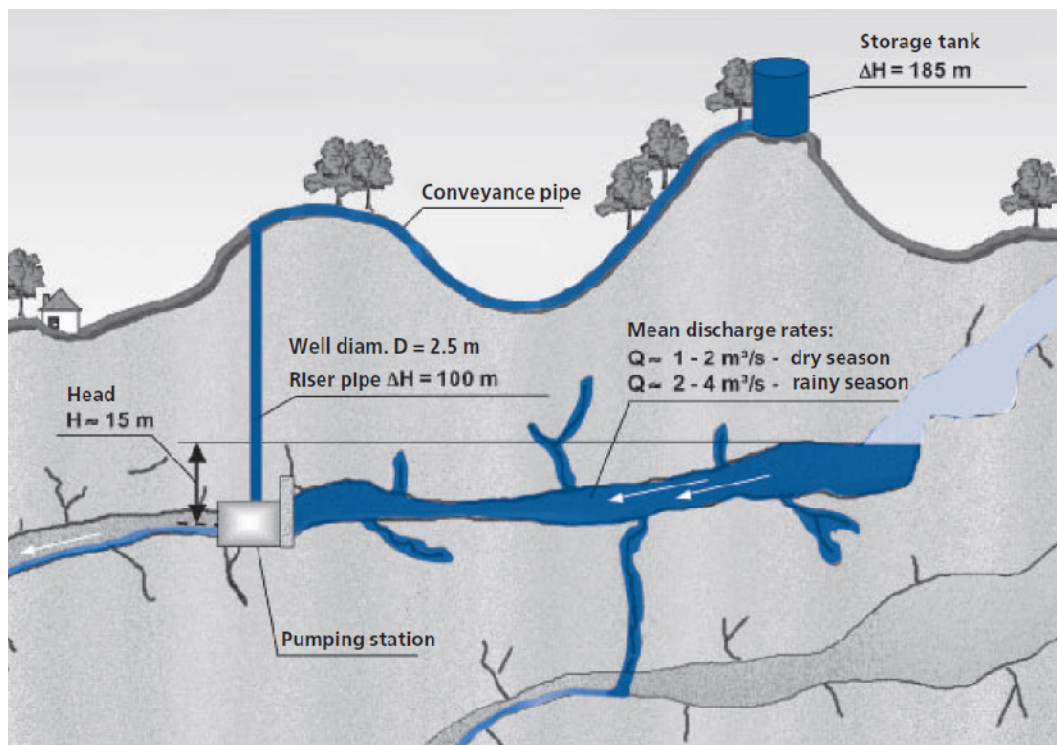


Figure 8: Linked shaft PAT/pump system in Java, Indonesia (Baumgarten & Guder, 2005)

The size of the pump was chosen based on the output power from the PAT and the head required. As the rotational speeds of the pump and PAT did not match, a gearbox was required between the shafts of the pump and PAT (Figure 9). During testing the system reached all its specified performance data and showed smooth and stable running behaviour at various duty points.

KSB do not currently sell off-the-shelf packages of this kind. On request they can engineer a complete solution that is optimized for the site but they were not able to provide a cost estimate of such a system at the time of this report.

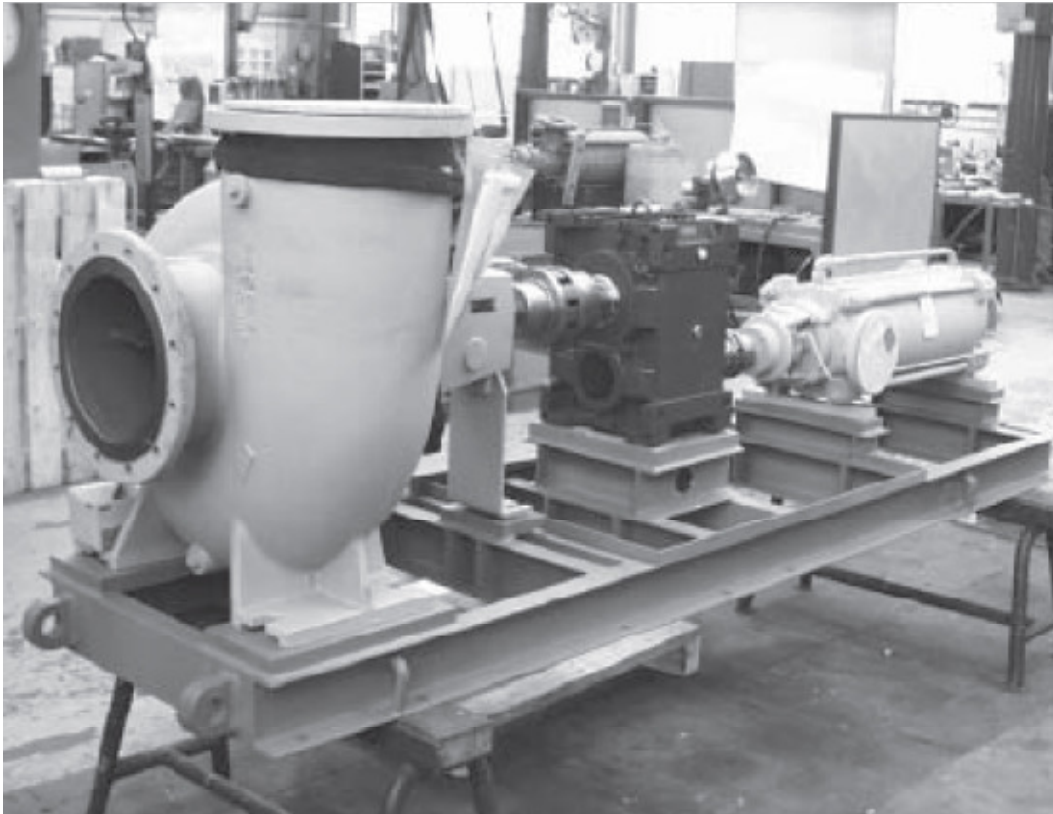


Figure 9: Assembled linked shaft PAT/pump system Indonesia (Baumgarten & Guder, 2005)

In normal grid-connected systems there is another aspect that should be taken into account. The so-called “feed-in tariffs” that are implemented in various countries provide compensation for renewable energy generated by Independent Power Producers (IPP) that is fed into the grid. The value of these feed-in tariffs is generally much higher than the cost at which the IPP would buy electricity from the utility. This means that using renewable energy on site when the feed-in tariff is available results in a loss of possible income. The South African REFIT rate for small hydro power is 0.94 R/kWh (NERSA, 2009). These tariffs will however not be taken into account for this project.

Maher et al. (1950) reports the installation of a double ended motor as generator in a hydro project. This provides a bare shaft to be used as a mechanical drive, while electricity is generated when the drive is not being used. This provides the efficiency of a linked-shaft system along with the flexibility of a generator system, albeit at a higher cost and increased system complexity. The maintenance intervals and breakdown frequencies of turbines and pumps are not however high enough to justify this cost in small scale projects.

3. COMPUTER SIMULATION

As the project requires many repetitive calculations in order to make the design choices, it was decided to develop a computer program that calculates the required parameters from user inputs. The function of the program is to reduce the time spent on calculations and provide repeatable, accurate results. The requirements of the program were:

- Provide accurate results
- User-friendly operation
- Fast calculations
- Capability to handle both frictionless flows and flows with friction
- Make provision for water salinity and temperature in density calculations

In order to make the program user-friendly, a GUI (Graphical User Interface) is used to communicate with the user. This leads to the decision to use C++/CLR as the programming language with Microsoft Visual Studio as the programming environment because GUI manipulation is very simple and easy to implement using this software.

To calculate the power output from the turbine, several properties are required as seen in equation 3.1.

$$P = \eta g \rho Q H \quad (3.1)$$

The turbine efficiency (η) varies for each different turbine and for the different operating conditions. For traditional turbines this can usually be determined from data supplied by the manufacturer which is often in graph format. For a PAT system the efficiency will have to be either calculated using the available pump curves from the manufacturer and one of the correlations found in the literature, or obtained through experimental procedures.

Gravitational acceleration varies slightly with position and altitude, but a value of 9.81 m/s^2 can safely be assumed in most cases. The density of the fluid is normally a function of temperature, but seeing as though the working fluid in this case is seawater the effect of the salt content of the water on density has to be established. The equations used in this case are given in Appendix A.

As the flow rate may vary considerably, the power output calculated should be seen as an instantaneous value which is only valid for the specified values. Even if an average flow rate value is entered the resulting power output is not

necessarily the average power output. This is due to the fact that the turbine efficiency is dependent on the flow rate, and pipe friction losses used in calculating the net available head are also dependant on flow rate. Thus there is an important design consideration to be made when varying flow rates are considered: if the turbine is designed for average flow rate it will sometimes be operating below its best efficiency point, which reduces its efficiency. At other times it will operate at higher flow rates which also reduce efficiency and can also damage the turbine. One method that can be used to avoid the fluctuations in the flow is to build a reservoir at the upper end of the penstock. This provides a buffer for when the flow rate increases and flow control is used at the turbine, and also backup for when the flow rate is lower than the average.

The difference in elevation between the turbine and the upper reservoir is called the “head”. Any losses in the pipe due to friction or viscosity are converted into an equivalent form and when subtracted from the head the result represents the “net available head”. The elevation difference can be determined from topographical maps or using GPS units. The head losses can come from a variety of sources and thus several equations have been developed to account for them (White, 2002). The losses are normally expressed in terms of a head loss coefficient which is then used in tandem with equation 3.2 to calculate the resulting head loss.

$$h_{loss} = k \left(\frac{v^2}{2g} \right) \quad (3.2)$$

The first head loss that is considered is friction losses in the pipe. This is normally given in graphical format in the so-called Moody chart, but for the purposes of this program an equation is required. The friction factor is highly dependent on the Reynolds number of the flow, given in equation 3.3.

$$Re = \frac{dv}{\nu} \quad (3.4)$$

If the Reynolds number is below 2100 it can be assumed that laminar flow is occurring, in which case the friction factor is simply:

$$f = \frac{64}{Re} \quad (3.5)$$

If the Reynolds number is above this value there is a transitional period where it is not certain whether fully laminar or turbulent flow is occurring. In this case turbulent flow is assumed and the applicable equation is:

$$f = \frac{1.325}{\left(\log \left(\frac{e}{3.7} + \frac{5.74}{Re^{0.9}} \right) \right)^2} \quad (3.6)$$

In this equation the pipe roughness factor (e) is required. This is found in Table 3.

Table 3: Values of pipe roughness for various materials

Material	e (mm)
Drawn tubing, brass, lead, glass, bituminous lining	0.0015
Commercial Steel or Wrought Iron	0.046
Welded steel pipe	0.046
Galvanized Iron	0.15
Concrete	0.3-3
Riveted Steel	0.9-9

When the friction factor is know it is simple to calculate the friction head loss coefficient using equation 3.7.

$$k_{friction} = f \left(\frac{L}{D} \right) \quad (3.7)$$

There are also certain losses that occur at the pipe entrance. The losses occur as a result of the contraction and subsequent expansion of water stream lines flowing into the pipe section. Several values for the entrance loss coefficient have been experimentally determined and are given in Figure 10.

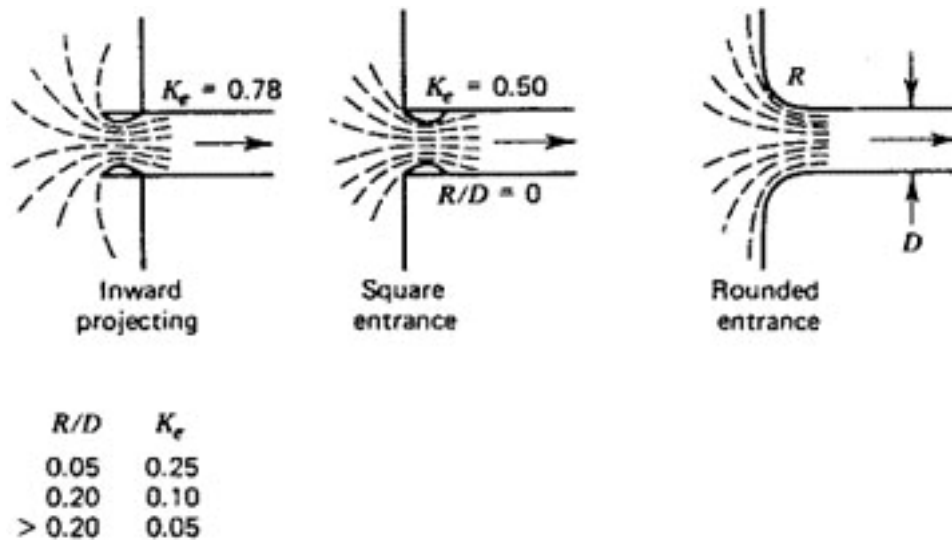


Figure 10: Inlet loss coefficients

Some commonly encountered pipe sections also induce losses in the system. The head loss coefficients for these pipe sections are given in Table 4.

Table 4: Head loss coefficient for various pipe segments

Fitting	$k_{sections}$
Gate Valve (wide open)	0.19
Gate Valve (half open)	2.06
Long radius bend	0.6
Short radius bend	0.9
T (through side outlet)	1.8
Smoothly curved contraction	0.05

The total head loss can now easily be calculated from equation 3.8 by using the head loss coefficient for each entrance, pipe section and pipe material.

$$h_l = \left(\sum k_{friction} + \sum k_{entrance} + \sum k_{sections} \right) \left(\frac{v^2}{2g} \right) \quad (3.8)$$

This means that all required parameters are available and the power output from the turbine can be calculated using equation 3.1.

It was decided to use a summation algorithm that first calculates the speed in the pipe for the given flow rate without any friction losses and then calculates the head loss coefficients from this value. This is a valid assumption because the flow rate is governed by mass continuity and should thus be unaffected by these losses. The procedure for this program is thus as follows:

1. Enter the various input values
2. Press the “calculate” button to determine the flow velocity (and the power output without any losses)
3. Use the head loss panel to add any components one at a time
4. The total head loss will now display and a press of the “calculate” button will determine the new power output

The program runs very fast due to the simple calculations and is very easy to use expect for the head loss values which require a basic understanding of the way in which they work. The program was tested on both Windows XP and Windows 7 and worked on both operating systems. The results were checked against hand calculations and were correct for a variety of solutions. A screenshot of the program is given in Figure 11.

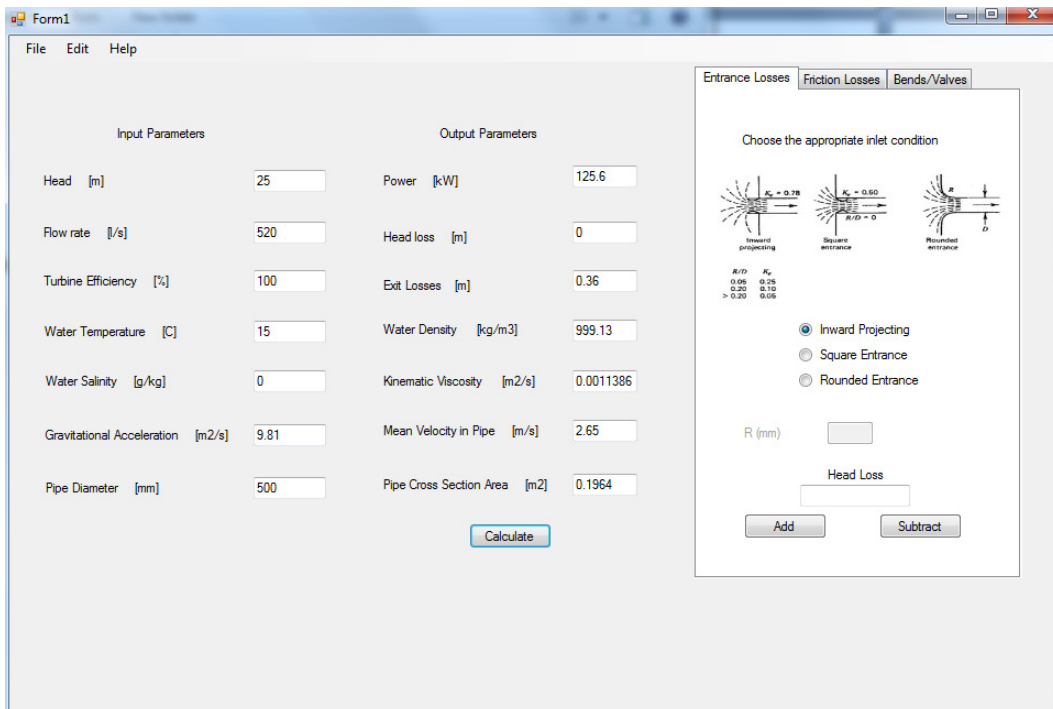


Figure 11: Screenshot of the simulation program

4. CURRENT SETUP AND FUTURE EXPANSION AT ROMAN BAY

A map of Roman Bay Sea Farm is shown in Figure 12. The map shows the inlet and outlet pipes, as well as the location of the current and future pump sheds. Some altitude information is also provided.

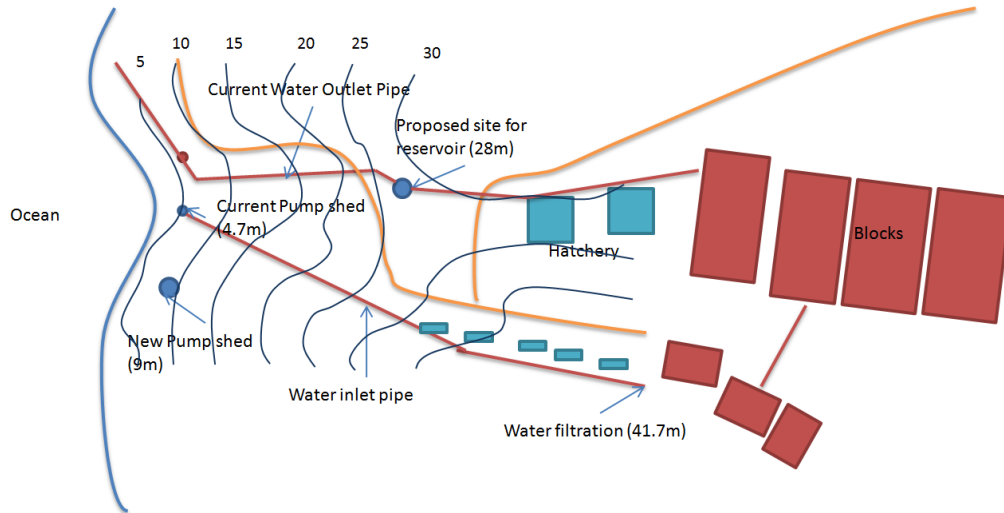


Figure 12: Map of Roman Bay showing important areas

4.1 Pump models and average flow rate

There are currently four pumps running constantly in order to supply water to the farm. The pumps are powered by four 110 kW motors, for a total of 440 kW. The pump models and average water pump rate (according to Angelo Bucchianeri from Roman Bay Sea Farm) are as follows in Table 5.

Table 5: Pump flow rates

Manufacturer	Model	Flow rate (l/s)	Number of pumps	Total flow rate (l/s)
KSB	200-610	170	1	170
Rapid Allweiler	200-400	130	3	390
Total				560

As all of this water is returned to the sea this is also the flow rate in the returning pipes. The outlet water flow is shown in Figure 13.



Figure 13: Outlet water flow

4.2 Outflow

Most of the water flows through two pipes which are combined into one pipe before a biofilter. These are low pressure pipes and thus cannot be used for the turbine. After the biofilter the water flows out into a channel (Figure 14) and then on to the ocean. It is important that the outlet water flow is not close to the inlet in order to avoid mixing the two flows and thus degrading the water quality.

Some of the water flowing through the current pipes is used to supply a blood worm farm with water. The blood worm farm is currently located near the pump house.

4.3 Future expansion

Roman Bay is planning to increase the capacity of the pumps and then build a channel in order to transport the additional water away from the farm. The output of this channel is situated further away from the pump house in order to supply water for a future blood worm expansion.



Figure 14: Outlet water channel

The pump house will move further south into a new location as they are experiencing problems with the current intakes that are taking in too much sand and debris. The new location is situated in an area with a rocky base which should reduce this problem.

4.4 Proposed site to investigate

If all of the water flow could be sent through a high pressure pipe down to the pump station there is a theoretic power output (turbine efficiency 90%) of 110 kW before pipe losses, assuming a head of 20m. The head could be attained by building an intermediate reservoir at a point 28m above the outlet of the pipes and then building a high pressure pipe from there to the current pump house.

5. CONCEPT EVALUATION

The conclusion from the literature review and the current setup at Roman Bay Sea Farm is that a variety of systems can be considered for this project. This section gives a basic description of the setup and components of each system and the advantages and disadvantages of each. The purpose of this concept evaluation is to determine the system that would be most appropriate for the application.

Four concepts will be evaluated as to how well they fit the client specifications which are presented in Table 6 along with the equivalent measurable engineering specifications.

Table 6: Client and engineering specifications

Client Specification	Engineering Specification
Generate power from the returning flow of seawater	Supply: 520 l/s flow rate 23 m head
Use the power to pump water back to the farm	Deliver: 170 l/s 40 m head
Good efficiency	Turbine efficiency larger than 80% Less than 2 m total head loss in pipes
Quality	Design for a life cycle of 20 years
Safety	Pipes rated for a minimum of 3 bar pressure Fittings rated for a minimum of 3 bar pressure Electrical sub-systems insulated from water No exposed moving parts Filter all debris larger than 100 mm ²
Road must still be usable	No part of system to be on the road

Provide a small backup supply	400 m ³ reservoir coupled with existing dams
It must be possible to divert the water flow away from the turbine	No water must reach the turbine when a certain valve or switch is turned on
Low cost	Total capital cost less than R 1 000 000
Simple maintenance	Maintenance can be performed by unspecialised personnel Life cycle operation and maintenance cost of less than 10% of capital costs
Protect from environmental damage	Use corrosion resistant materials in pipe, fittings and turbine Bury pipe 30 cm underground Seal pump house from animals
Low environmental impact	Less than 200 m ³ earth moved Use existing structures where possible Replant any flora that is removed Do not use diesel generators for backup supply Use local manufacturers to limit shipping

The major choices that need to be made are highlighted in Figure 15. The components in dark blue are considered essential for any system and do not depend on the system configuration. The bypass valve is required for times when either the turbine/PAT or pump/generator is undergoing maintenance so that the water flow can be controlled.

The requirement of an upper reservoir is debatable as the water is already stored in holding tanks before the abalone blocks. The water does however split off into the various sections of the farm and thus a central meeting point for all the water flow toward the sea would simplify the system. It also provides a good centre to clean the water. The water flow is expected to be free of any major debris such as sticks, stones or leaves due to the usage of the water in the farm. This removes the need for complicated filters or mulchers in the upper reservoir. A simple wire mesh filter should remove any significant dangers and the water outlet should be located above the bottom of the reservoir to avoid debris build-up.

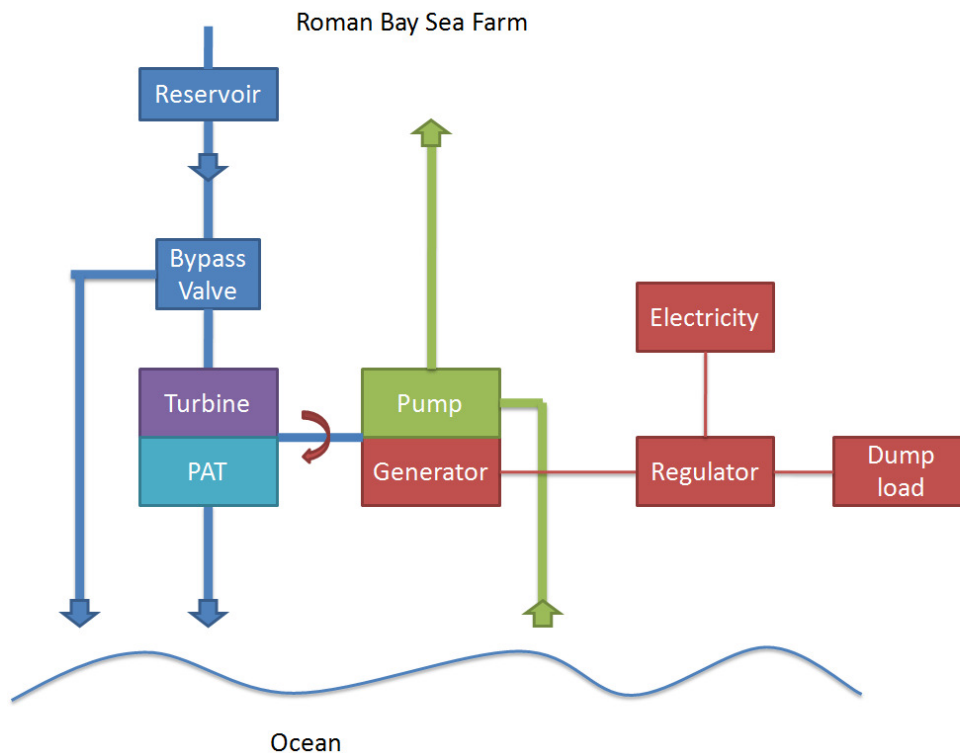


Figure 15: Overview of design decisions to be made

The first major choice is whether to use a traditional turbine or a PAT system and the second major choice concerns the utilization of the shaft power gained from the turbine/PAT. This leads to four possible concepts for the project which are shown in Figure 16.

Concept A is a traditional turbine that provides mechanical power on its output shaft. This mechanical power is transferred to an existing pump through a direct drive couple system.

Concept B is the conventional method that is used in most microhydro systems. It uses a traditional turbine to power a generator which provides electricity as an

output. The electricity is then used to power one of the existing pumps and a regulator is required in order to manage the load.

Concept C is the same as concept A, but in this case the traditional turbine is replaced by a centrifugal pump operating in reverse. Concept D is the same as Concept B, but again the traditional turbine is replaced by a PAT.

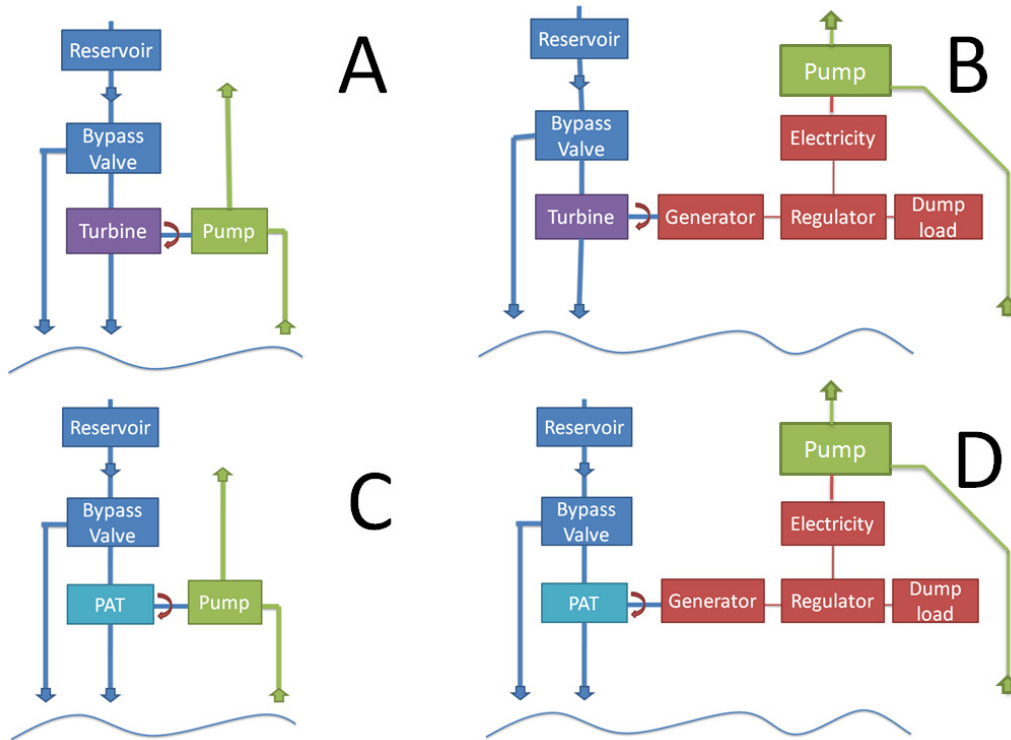


Figure 16: The four different concepts considered for this project

The two main choices can be made virtually independently as they do not have any significant influence on each other. Thus the first selection is the power-generating device and the second is the power consuming device.

There are two possible ways to design the driven pump section of the system if it is decided to continue with the direct-drive system. Either purchase a new pump that operates at values close to the output parameters of the turbine/PAT, or determine whether one of the existing pumps can be powered. The second option would be considered ideal from a cost-effectiveness viewpoint, while the first could possibly result in a better total efficiency. The advantages and disadvantages of each choice are given in Table 7.

Table 7: Advantages and disadvantages of the two direct-drive system pump choices

	Existing Pump	New pump
Advantages	Cost-effective	Probable higher efficiency by operating at BEP
		Could reduce peak pumping load
		No gearbox required
Disadvantages	Probable loss in total pumping power by operating pump away from BEP	More expensive
	May require gearbox	
	Requires pump to operate in similar power range as PAT output	

The disadvantages of the existing pump setup can be avoided if the existing pumps are in the correct operating range and then the costs of a new pump are avoided.

In order to facilitate the design choices, we require a measure of cost-effectiveness versus energy output for each system so that direct comparisons can be made. This is done by taking the total cost of each concept and dividing it by the total usable energy recovered from each system. The result is a Rand per kilowatt-hour value that incorporates the two main specifications.

Firstly the total cost of each system must be determined. From Figure 2 it is clear that the chosen site makes various turbine types suitable to the application and thus the estimates that could be obtained were for three different types of turbines. The cost prediction formulas of Ogayar and Vidal (2009) also provide a way to determine which type of turbine would be the most cost effective for this site. Using a net head of 23 m and a power of 100 kW the predicted initial capital costs of the electro-mechanical equipment for this project can be compared in Table 8.

Table 8: Cost prediction results

Turbine	Initial Capital Cost of electro-mechanical equipment (Euro/W)	Rand Equivalent (08-10-09)
Pelton	1.42	R 15.50
Francis	1.33	R 14.40
Kaplan	1.61	R 17.40
Semi-Kaplan	0.94	R 10.20

While the absolute values may not hold much value as the formulas were not based on data from South African sites, the relative values show that a semi-Kaplan turbine should be the most cost-effective non-PAT solution in this case.

No local suppliers could be found that were able to supply an estimate of the costs of a suitable turbine and as such the only estimates that could be obtained are from international manufacturers. KSB do however have a South African branch and thus the estimate does not need to be adjusted for international shipping. These turbines all operate with a BEP in the range of 520 l/s and 23 m head, and have varying power outputs depending on the turbine efficiency. These devices are all suitable for use with seawater. The estimates were as follows:

Table 9: Estimates of turbine costs for various systems

Manufacturer	Type of Turbine	Designation	Type of Quote	Price	Rand Equivalent (08-10-09)
KSB	PAT	Omega 350-510A	Bare Shaft	R 210 000	R 210 000 ex. VAT
Cargo & Craft	Turgo	Unknown	Water to wire	€ 149 000	R 1.62 mil ex VAT
Gilkes	Francis	425 G150	N/A	Could not be obtained	N/A
Evans Engineering UK	Pelton	Unknown	Water to wire	£ 50 000	R 591 559 ex. VAT

Gilkes reported that they would not be competitive on price at the parameters of the chosen site and thus for the turbine-generator solution (concept B) the Evans Engineering UK estimate is used as the total cost of the electro mechanical equipment. The cost of the turbine without the generator and regulating equipment was not available, and thus it was assumed that the electrical sub-system costs in the order of R 165 000, bringing the cost of just the turbine to R 426 000. This is then the total cost of Concept A.

Concept C only requires the KSB PAT and some coupling devices, whereas Concept D requires an additional generator and regulating equipment (sourced from Grootplaas Engineering and Irrigation) for R 165 500.

Furthermore, the total efficiency of each system must be determined in order that the total power output can be calculated. The efficiency of the turbine and PAT respectively is 83% and 87%. The efficiency of the generator is assumed to be 85% as this is the value used by Evans Engineering UK. Transmission over a short range is 98% and the motor used to power the pump is assumed to be 85% efficient as well. The pump that is powered has the same efficiency for all cases and is thus not used in these calculations. The total efficiency of each system can now be determined and is given in Table 10 along with the total costs of the electro-mechanical equipment for each concept. The electro-mechanical equipment includes the turbine (or PAT), generator and any electrical regulating devices used. The usable power is the total power that is delivered to the existing pump in each case.

Table 10: Cost per installed kilowatt of electro-mechanical equipment

Concept	Cost (R)	Total Efficiency (%)	Usable Power Output (kW)	Cost/power output (R/kW)
A	426 000	83	95.5	4 463
B	591 559	59	67.9	8 719
C	210 000	87	100	2 099
D	375 500	62	71.3	5 266

From a capital investment viewpoint for the electro-mechanical sub-system Concept C shows the lowest cost per kilowatt. A more appropriate measure would be to determine the cost per kilowatt-hour of each system and compare this with the cost of electricity from Eskom. This requires a measure of the total operation and maintenance (O & M) costs of each system in order that the total life-cycle costs can be determined. Vaidya (s.a) inspected various microhydro sites and found that the total O & M costs over the life cycle of the plants varied between 5% and 14% of the initial investment. As Roman Bay Sea Farm already has four operating pumps that have to be maintained it is assumed that O & M costs for this project will be on the lower side of the range, especially if a PAT is used.

Using a life-cycle O & M value of 7% of the initial capital investment, the total capital costs for each concept and an assumed interest rate of 10%, the total cost of each concept over the predicted life cycle of the project (twenty years) can be determined. This is shown in Table 11.

Table 11: Total costs of each concept (ex VAT)

	Electro-Mechanical (R)	Civil (R)	O & M (R)	Yearly Instalment (R)	Total Cost of Capital (R)	Total Costs
A	426 000	191 862	43 250	72 573	1 451 476	R 1 494 727
B	591 559	191 862	54 839	92 020	1 840 406	R 1 895 246
C	210 000	191 862	28 130	47 202	944 051	R 972 181
D	375 500	191 862	39 715	66 642	1 332 842	R 1 372 557

The total cost is then divided by the total predicted energy that will be supplied over the life cycle in order to determine the cost per kilowatt-hour for each concept. In predicting the total energy supplied an availability factor of 95% was used, which Vaidya (s.a.) recommended. The cost per kilowatt-hour value that results provides an ideal way to compare the projects to each other and to Eskom prices.

Table 12: Total cost per kilowatt-hour for each concept

Concept	Total Costs	Total Power (kW)	Total Energy (kWh)	Cost per kWh
A	R 1 494 727	95.5	15 895 020	R 0.09
B	R 1 895 246	67.9	11 301 276	R 0.17
C	R 972 181	100	16 644 000	R 0.06
D	R 1 372 557	71.3	11 867 172	R 0.12

Thus, concept C is quite clearly the most cost-effective and efficient solution, and also has the highest usable power output. Also, the concept will provide usable energy at a cost less than the equivalent that is provided from Eskom.

It should be noted that in this analysis a quote from a local manufacturer was competing against a quote from a London-based manufacturer. As such, the results may be skewed in the favour of the KSB pump, but this underlines the fact that pumps are much easier to source locally than turbines.

6. SYSTEM DESIGN

The chosen concept thus looks as follows in Figure 17. It now remains to determine the engineering specifications of the complete system, most notably the PAT and direct drive sub-systems.

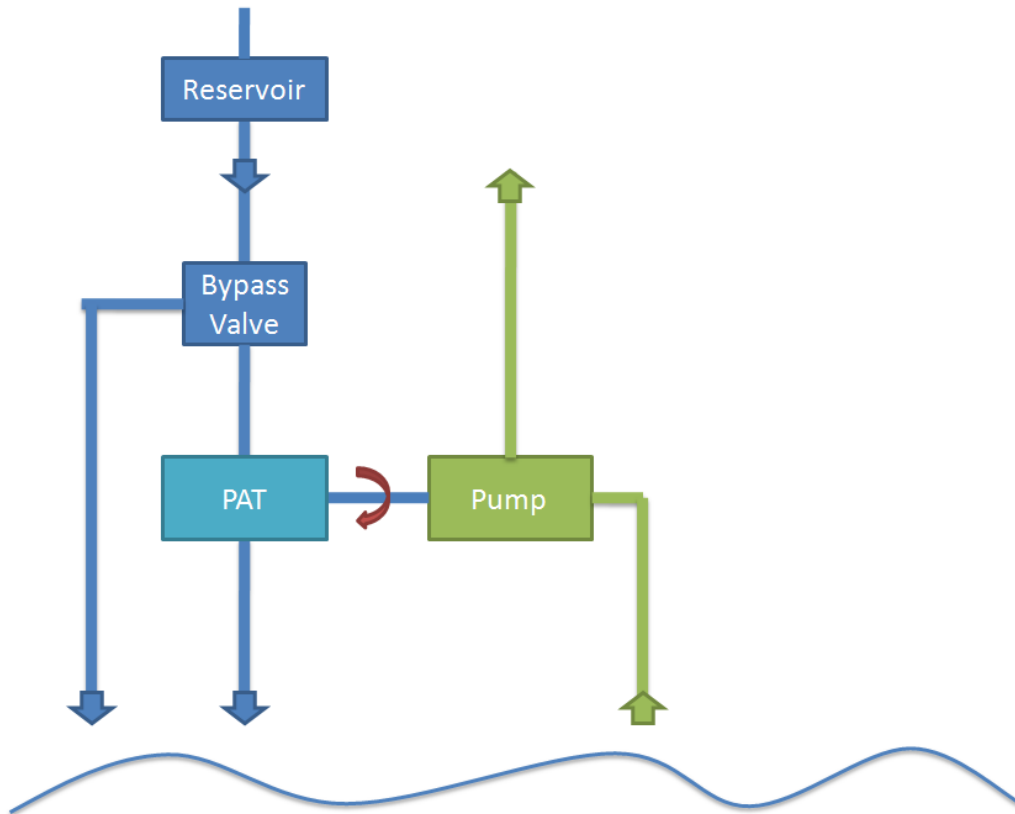


Figure 17: Concept design of system

6.1 Turbine selection

KSB was the only pump manufacturer that was able to supply data on their pumps operating as turbines. A suitable PAT was recommended by KSB, and the operating curves in both turbine and pump mode were supplied (Appendix F). This provides an ideal opportunity to test the accuracy of the correlations listed in Chapter 2.

The experimentally determined pump and turbine curves were read into MATLAB where the Best Efficiency Point (BEP) in both cases was determined. The pump BEP was then used to determine the predicted turbine BEP using all of the correlations so that they can be compared to the real (experimentally determined) BEP. The results were as follows in Figure 18.

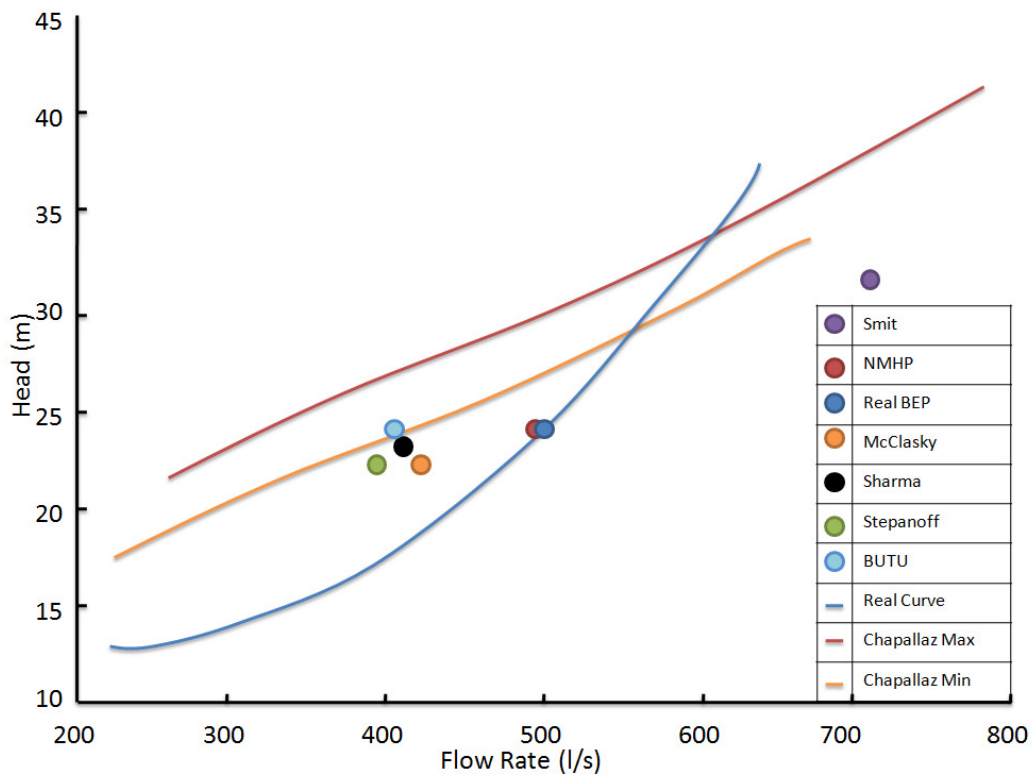


Figure 18: Correlation results versus experimental results

Most of the correlations predict two variables, namely the head and flow rate at BEP. The only method to predict the performance away from the BEP (Chapallaz, et al. 1992) gives a range of values for the head at various flow rates, but except for a small portion it is mostly inaccurate.

In order to assess the other correlations better, the error is given as percentage of the predicted value to the actual value for both the head and flow in Figure 19. It is clear that the method of Nepal Micro Hydro Power (2005) provides the most accurate results for this case. But as the method does not use any properties of the pump to calculate this value it is presumed that this close correlation is either coincidental, or that the author based the correlation on very similar pumps. This is quite clear in Smit (2005) where the same method was attempted and very different factors were found.

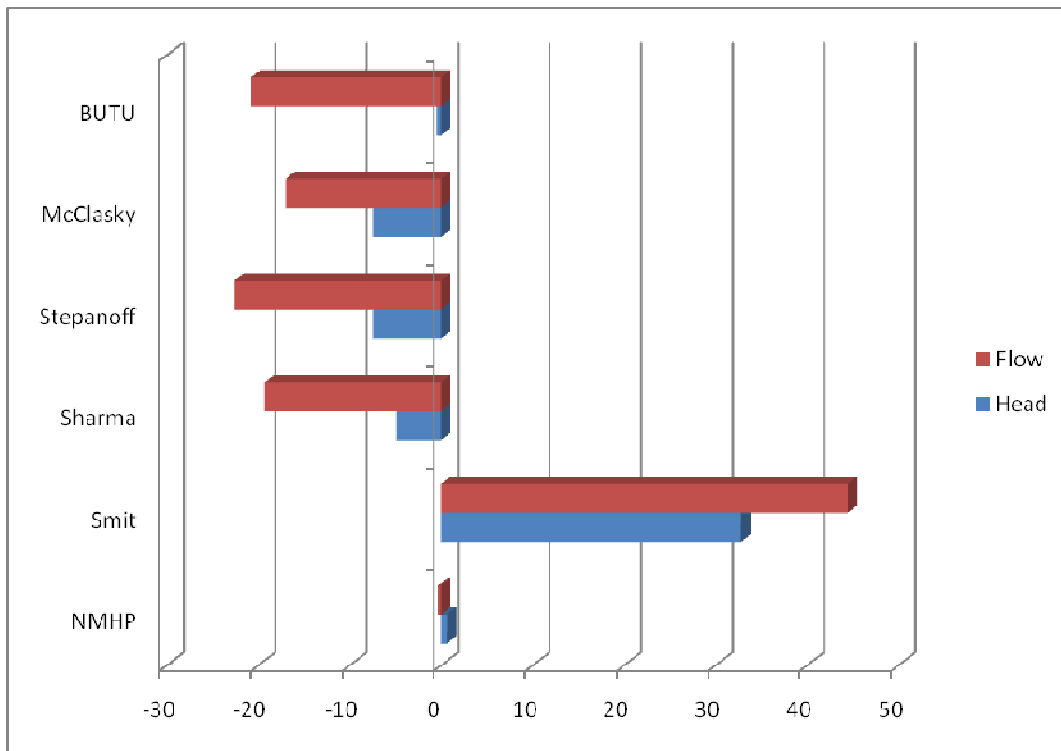


Figure 19: Percentage error in correlation flow and head

For the remaining methods, the head at BEP is predicted well (within 92% of the actual value for all correlations) and the flow rate at BEP less accurately (from 77% to 83% of actual value). The BUTU method shows the best result for head and McClasky the best for flow rate.

As these correlations are only tested for one specific pump in this case, the results of this test are inconclusive. In order to gain a better picture of the accuracy of the various methods this test should be done for a variety of different pumps. The one concrete conclusion is that no correlation can currently predict, with a high degree of reliability, turbine mode performance from pump curves. This means that in systems where the output parameters are critical, such as this project (the output rotational velocity has to be known in order to determine whether a gearbox is required for the direct drive system), the only reliable method is to use experimentally determined turbine-mode curves.

This does limit the choice of manufacturers substantially, as for this project the only manufacturer that had experimentally determined turbine-mode curves was KSB. The alternative is to use the correlations to predict a viable pump for the PAT system and then run experiments to determine the output parameters (power, BEP, specific speed) from which the driven pump can then be chosen,

but this means that the PAT will probably operate away from its BEP resulting in lower efficiency. The safer option (albeit at a possible cost premium) is thus to use the KSB PAT recommendation.

The output parameters from the PAT (as determined by KSB) are as follows:

Mechanical Power:	97 kW
Rotational Velocity:	741 rpm
Torque:	1250 Nm

6.2 Driven pump section

The pumps at Roman Bay Sea Farm are powered by 110 kW motors, and one of the pumps is manufactured by KSB. The probable input mechanical power to the pump is thus between 93 kW and 105 kW, depending on the efficiency of the motor. This is right in the range that the PAT will supply. The only restricting parameter is thus the rotational velocity of the pump as this might make the use of a gearbox necessary.

The operating curve of the KSB 200-610 pump currently in use at Roman Bay Sea Farm is given in Figure 30 in Appendix F. If this pump is powered by the PAT at 97 kW and 740 rpm it will operate at 82% efficiency, which is just below its BEP at 84%. Using the current known operating parameters of the pump (flow rate of 170 l/s and head of 40 m) it can be seen that the pump is already operating at a similar efficiency, and thus the pumping should not be affected by the change in input power.

The PAT can be used to power the existing KSB 200-610 by direct coupling of the shafts without the use of a gearbox, without any significant loss in hydraulic power.

6.3 Specification of remaining components

The components that remain to be specified are the reservoir, pipe system, pump house and valve system. These components are mostly standard parts that can be sourced from local suppliers.

The location of the outlet is constrained to the location of the current pumps. As the pumps are being moved to a new location, the outlet should also change location. However, the new location is 5 m higher than the old location and would thus result in a 25% loss in head. As such, it is recommended that one of

the pumps is moved back to its original position so that it can be powered directly by the PAT system

The upper reservoir can be built above ground with an intake that is connected to the outlet from the farm. The outlet of the reservoir is to be situated 1 m above the bottom and covered with a wire mesh in order to protect the turbine from sediments that can build up in the reservoir. In addition to this, measures must be taken for situations where the pipe can become blocked and overflow occurs. This is done by channelling the surface water to the existing water pipe whenever it reaches a certain level. Figure 20 shows a front isometric view of the proposed reservoir.

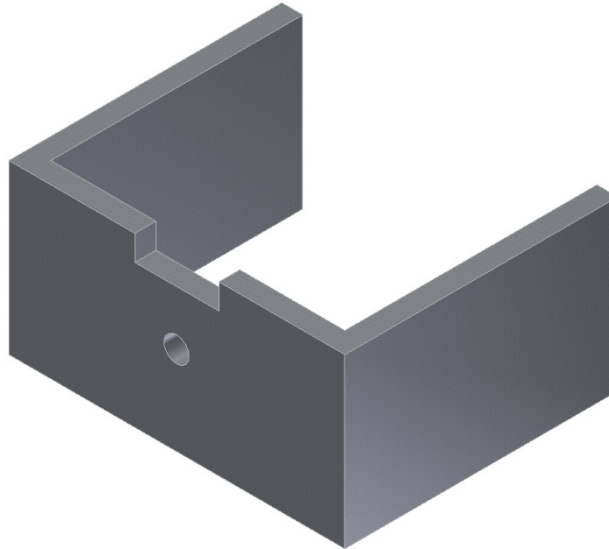


Figure 20: Reservoir Diagram

The pipe is sourced from Gast International SA (Pty) Ltd and is designated as “315mm PN05 SDR33 PE100 HDPE Pipe Plain Ended”. It is a 315 mm inner diameter HDPE pipe that is rated for 5 bar pressure. Delivery time is three to four weeks and 200 m of pipe is required for the project. The pipe is also used in order to direct the water in the preferred direction in which it should enter the turbine and as the turbine in this case is actually a pump operating in reverse, the penstock will be connected to the pump’s outlet which will be pointing upwards.

The pipe has a wall thickness of 12.1 mm. The hoop stress formula in equation 6.1 provides a measure of the maximum stress in the walls of the pipe.

$$\sigma_{\theta} = \frac{Pr}{t} \quad 6.1$$

Using a maximum expected water pressure of 3 bar (without surges), it is possible to find the hoop stress as 3.9 MPa. The tensile strength of HDPE varies, but a lower value of 22 MPa can be assumed according to Corneliusen (2002). This means that for the maximum expected pressure the chosen pipe has a safety factor of 5.6, which is more than enough to cover for any unexpected surges.

The existing pump house has been cleared of pumps and it is recommended to make use of the pump house for this project. This eliminates the need to build a separate structure specifically for this project.

Lastly, a gate valve is required to isolate the turbine from the water flow when required. The valve can be sourced from KSB as well and its designation is ZXS 300. When the gate valve is closed maintenance can be performed on the turbine. The water will then go through the overflow part of the upper reservoir into the old outlet pipe from where it will reach the ocean.

A schematic of the final system is shown in Figure 21 with the major design choices as well as the power after each section.

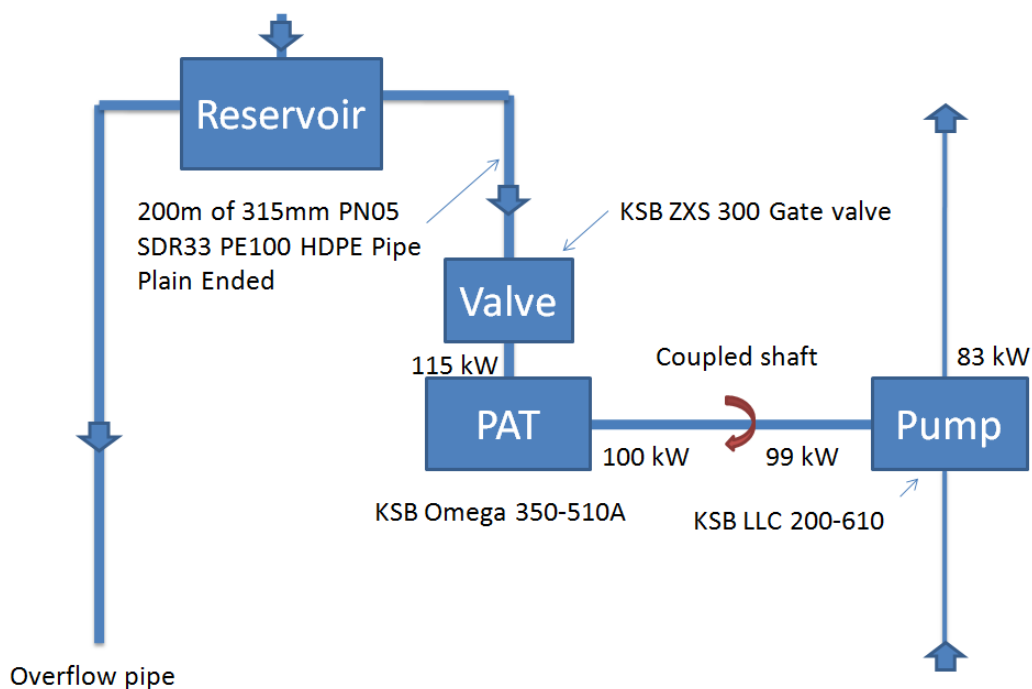


Figure 21: Schematic of final system

The setup inside the pump house will look as follows in Figure 22.

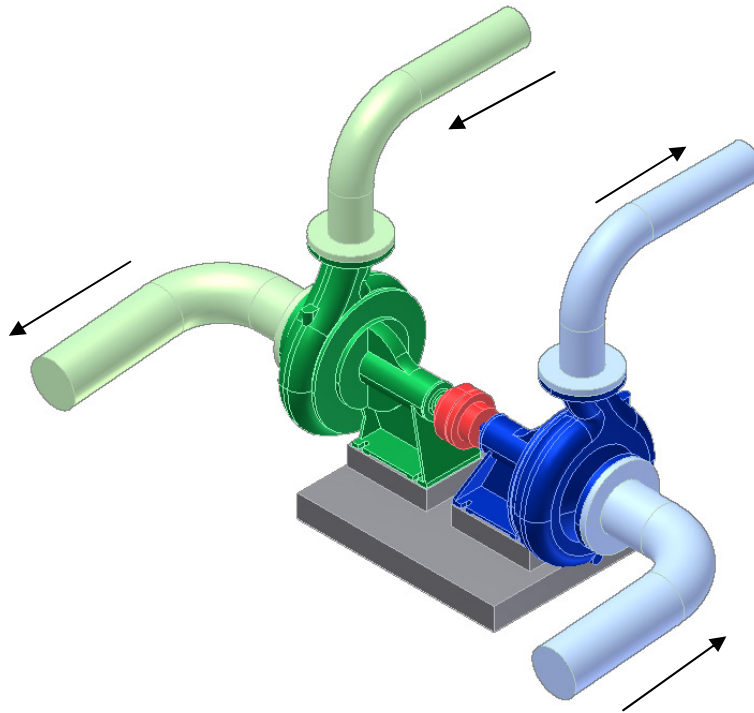


Figure 22: Setup inside pump house

The water enters the pump house through the green pipe where it is directed to the green centrifugal pump that is operating as a turbine. The PAT generates mechanical shaft power and the water flows out towards the ocean through the green pipe. The mechanical power from the output shaft of the green PAT is used to power a different model centrifugal pump (the blue pump in the diagram) by direct coupling of the shaft. This takes water from the ocean and pumps it back up to the farm using the blue pipe. It is important that the outlet pipe and the inlet pipe be situated away from each other so that the inlet pipe does not take up water that has already been through the farm.

7. PROJECT COSTS

The costs for the project can be divided into two major sections, namely the electro-mechanical equipment and the civil works. The electro-mechanical equipment includes the PAT and any electrical governing systems that are used. The price obtained from KSB is used in these calculations. The civil works include the upper reservoir, the pipe system and a pump shed. The rough estimates of the costs are summarized in Table 13.

Table 13: Rough estimates of preliminary costs for complete system

Item	Supplier	Cost
Omega 350-510A PAT - Shipping from Germiston	KSB	R 210 000 R 10 000
ZXS - 300 Gate Valve	KSB	R 8 950
315mm PN05 SDR33 PE100 HDPE Pipe Plain Ended - Shipping from Rosslyn	Gast International SA (Pty) Ltd	R 36 450 R 4 000
400 m ³ Reservoir		R 80 000
Installation (2 technicians and 5 labourers for 10 days)		R 52 500
Total (ex VAT)		R 402 000

In order to determine whether this project should proceed, it is necessary to do a cost-benefit analysis to determine the financial viability. This is done by weighing the future electricity savings versus the input costs of the system by using a discount rate for savings in the future. The outcome from this analysis is the Net Present Value (NPV) which is the current value of the electricity savings minus the initial project costs. The NPV can be calculated for each year that the project operates and when NPV becomes positive the project is paid back in full and begins to generate profit. The time which passes before the NPV becomes positive is called the payback period of the project.

Roman Bay Sea Farm uses a variable tariff structure for their electricity bill. The cost of electricity depends on the time at which it is used, with different prices for peak, standard and off-peak times as defined in Figure 23.

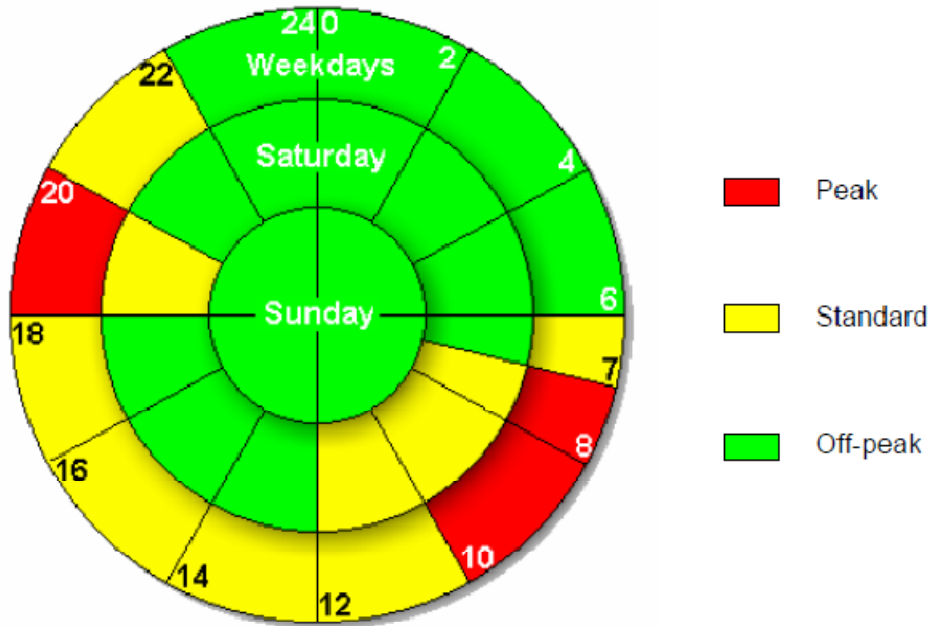


Figure 23: Eskom electricity tariff periods (Eskom, 2009)

The price which Roman Bay Sea Farm pays for electricity is given in Table 14.

Table 14: Roman Bay Sea Farm electricity prices (according to Angelo Bucchianeri from Roman Bay Sea Farm)

Period	Price (c/kWh)
Peak	55.45
Standard	34.34
Off-peak	24.32

Using these figures and a probable 97 kW constant mechanical power output from the PAT that replaces the 110 kW electrical motor currently used, it is possible to calculate the yearly electricity bill savings brought on by the installation of this system. It should be noted that this is not a precise value as public holidays influence the electricity tariff period, and also the system may be shut down for maintenance during the year.

For the first year, assuming electricity prices remain constant, the total monthly saving in the electricity bill is thus R 19 600. Assuming this value remains constant, which is an unrealistic scenario, the payback period of the project is 24 months. A worst-case scenario (for the end-user, but not for the financial viability of this project) is that Eskom receive the 35% yearly price increase that

they have applied for over the next three years (Waja, 2009). The new payback period then becomes twenty months. It is likely that the probable price increases will be somewhere between these two values and this clearly shows the dependence of the payback period on the electricity price. The project seems financially viable at present rates, and only becomes more favourable as the electricity price increases. After the initial payback period has passed, the total monthly savings can be regarded as income for the commercial operation for the lifetime of the system.

This analysis coupled with the cost per kilowatt-hour analysis done in the previous section proves that the project is viable even at present rates. This project should not however be measured on a purely financial basis as there are other advantages such as increased sustainability of the whole plant and the small backup supply that the system would provide. This, along with the likelihood of high future electricity prices, proves to make this project viable.

8. SUMMARY

This report covered the design process of a micro hydro development at Roman Bay Sea Farm in Gansbaai. It includes a literature study on micro hydro systems with a focus on Pump-as-Turbine technology which concludes that PAT can be a cost-effective alternative to traditional turbines as long as the turbine mode curves can be determined.

Several concepts are evaluated and a PAT system that is coupled to an existing pump is found as the most solution which fits the client specifications best. It is found that the most suitable concept can provide usable energy at a rate less than the current Eskom tariff. A computer simulation program was programmed to help with the design process and can be used in other hydro projects to save time.

The complete system is specified and first order estimates for the various parts are obtained. A cost-benefit analysis shows the financial viability of the project is dependent on the cost of electricity. With predicted future price increases being the main motivation for the project it can thus be concluded that the project is financially viable. In addition to this it will increase the sustainability of the farm and provide a small backup supply in case of a disruption in the grid connection.

In order to proceed from here, official quotes should be obtained from the manufacturers in order to set up a more detailed budget. The next step for Roman Bay Sea Farm is thus to evaluate this proposal in order to determine whether to continue with the project.

9. REFERENCES

- Alatorre-Frenk, C. 1994. *Cost minimization in microhydro systems using pumps-as-turbine.*, Ph.D.M.E. Thesis. University of Warwick
- Aronson, J. 2008. *Water Rites: A Microhydro Evolution.* Home Power 122. (Online). Available: www.homepower.com (15-09-09)
- Baumgarten, S. and Guder, W. 2005. *Pump as Turbines.* Techno digest No. 11. KSB Aktiengesellschaft
- Chapallaz, J. M., Eichenberger, P. and Fischer, G. 1992. *Manual on Pumps Used as Turbines.* Volume 11. Deutsches Zentrum fur Entwicklungstechnologien GATE
- Corneliussen, R. 2002. *Properties: High Density Polyethylene (HDPE).* (Online) Available: www.maropolymeronline.com (09-12-09)
- Cunningham, P. and Woofenden, I. 2007. *Microhydro-Electric Systems Simplified.* Home Power 117. (Online). Available: www.homepower.com (15-09-09)
- Derakhshan, S. and Nourbakhsh, A. 2007. *Experimental study of characteristic curves of centrifugal pumps working as turbines in different specific speeds.* Experimental Thermal and Fluid Science 32 800–807
- Derakhshan, S. and Nourbakhsh, A. 2008. *Theoretical, numerical and experimental investigation of centrifugal pumps in reverse operation.* Experimental Thermal and Fluid Science 32 1620–1627
- Eskom. 2009. *Tariffs and charges 2009/10.* (Online). Available: http://www.eskom.co.za/live/content.php?Category_ID=26
- Kaya, D., Alptekin Yagmur, E., Suleyman Yigit, K., Kilic, F.C., Salih Eren, A. and Celik, C. 2008. *Energy efficiency in pumps.* Energy Conversion and Management 49 1662–1673
- Maher, P., Smith, N.P.A. and Williams, A.A. 2003. *Assessment of pico hydro as an option for off-grid electrification in Kenya.* Renewable Energy 28 1357-1369
- McCutcheon, S.C., Martin, J.L, Barnwell, T.O. Jr. 1993. *Water Quality in Maidment.* Handbood of Hydrology, McGraw-Hill, New York, NY (p. 11.3)

- Meyer, A.J., and Van Niekerk, J.L. 2008. *Renewable Energy Study for Roman Bay Sea Farm: Final Report*. Centre for Renewable and Sustainable Energy Studies, Stellenbosch University
- Mills, A.F. 1999. *Heat Transfer*. Prentice Hall Inc. Upper Saddle River, NJ.
- Nepal Micro Hydro Power. 2005. *Pump-as-turbine technology*. Intermediate Technology Development Group. September 29
- NERSA. 2009. *South African Renewable Energy Feed-in Tariff (REFIT): Regulatory Guidelines 26 March 2009*. Pretoria: NERSA
- Ogayar, B. and Vidal, P.G. 2009. *Cost Determination of the Electro-Mechanical equipment of a small hydro-power plant*. *Renewable Energy* 34 6-13
- Pigaht, M. and van der Plas, R.J. 2009. *Innovative private micro-hydro power development in Rwanda*. *Energy Policy* (2009)
- Rawal, S. and Kshirsagar, J.T. 2007. *Numerical Simulation on a Pump Operating in a Turbine Mode*. Proceedings of the Twenty-Third International Pump Users Symposium
- Sharma, K. 1985. *Small hydroelectric project-use of centrifugal pumps as turbines, Technical Report*. Kirloskan Electric Co. Bangalore, India
- Smit, E.N. 2005. *Micro Hydro Power Generation*. Final Year Project Report. Faculty of Engineering, Stellenbosch University
- Stepanoff, A.J. 1957. *Centrifugal and Axial Flow Pumps, Design and Applications*. John Wiley and Sons, Inc. New York
- Vaidya. s.a. *Cost and Revenue Structures for Micro-Hydro Projects in Nepal*. (Online). Available: www.microhydropower.net/download/mhpcosts.pdf (04-12-09)
- Waja, R. 2009. *Eskom adjusts its Tariff Increase Application to Nersa*. (Online). Available: www.sacci.org.za (09-12-09)
- Western North Carolina Renewable Energy Initiative. 2007. *Fact Sheet: Microhydro*. Appalachian State University
- White, F.M. 2002. *Fluid Mechanics: fifth edition*. McGraw-Hill, New York, NY

Williams, A.A. 1996. *Pumps as turbines for low cost micro hydro power*. World Renewable Energy Conference, June 1996. Denver, USA

APPENDIX A: FLUID PROPERTY DETERMINATION

In order to calculate the power output from the turbine in Section 6, several fluid properties are required. The first and most important property is the density (ρ) of the fluid. McCutcheon et al. (1993) provide data that shows the density of water for different temperatures and salinity levels. The density as a function of temperature is given in equation A-1.

$$\rho(T) = 1000 * \left(1 - \frac{T + 288.9414}{508929.2(T + 68.12963)} (T - 3.9863)^2\right) \quad \text{A-1}$$

The effect on density of salinity is then quantified by equation A-2.

$$\rho(T, S) = \rho(T) + aS + bS^{\frac{3}{2}} + (4.8314 \times 10^{-4})S^2 \quad \text{A-2}$$

With

$$a = 0.824493 - 0.0040899T + (7.6438 \times 10^{-5})T^2 - (8.2467 \times 10^{-7})T^3 + (5.3675 \times 10^{-9})T^4$$

$$b = -(5.724 \times 10^{-3}) + (1.0227 \times 10^{-4})T - (1.6546 \times 10^{-6})T^2$$

Kinematic viscosity is used in the calculation of the Reynolds number and is calculated by a fifth order polynomial fit through the values found in Mills (1999). The resulting equation for kinematic viscosity as a function of temperature is given in equation A-3.

$$\nu = ((-3.946 \times 10^{-10})T^5 + (1.311 \times 10^{-7})T^4 - (1.7698 \times 10^{-5})T^3 + (1.294 \times 10^{-3})T^2 - 0.05898T + 1.7855)/1000 \quad \text{A-3}$$

APPENDIX B: TURBINE COST PREDICTION FORMULAS

The equations given by Ogayar and Vidal (2009) predict the cost per kW for various common turbines over a range of power output under 2 MW.

Pelton Turbines

$$COST = 17.693P^{-0.3644725}H^{-0.281735} \quad (B-1)$$

Francis Turbines

$$COST = 25.698P^{-0.560135}H^{-0.127243} \quad (B-2)$$

Kaplan turbines

$$COST = 19.498P^{-0.58338}H^{-0.113901} \quad (B-3)$$

Semi-Kaplan turbines

$$COST = 33.239P^{-0.58338}H^{-0.113901} \quad (B-4)$$

The preceding equations were found to have an error ranging between approximately +20% and -20%.

APPENDIX C: BUTU METHOD FOR PREDICTING PAT PERFORMANCE FROM PUMP PERFORMANCE DATA

The BUTU (referring to the acronym of “Pump as Turbine” in Spanish) method was initially developed in Mexico before being completed in Great Britain. It provides empirical curve fits and the accuracy is reported to be within 10%.

Firstly the performance at BEP is calculated using the following formulas:

$$\frac{P_{rp}}{P_{rt}} = 2\eta_p^{9.5} + 0.205 \quad \text{C-1}$$

$$\frac{H_{rp}}{H_{rt}} = 0.85\eta_p^5 + 0.385 \quad \text{C-2}$$

$$\eta_{rt} = \eta_{rp} - 0.03 \quad \text{C-3}$$

Now the rest of the curve can be calculated by using equation C-4 in conjunction with C-5 and C-6, and then substituting into equation C-7.

$$\frac{P_t}{P_{rt}} = (1 - k) \left(\frac{Q_t}{Q_{rt}} \right)^2 + k \frac{Q_t}{Q_{rt}} \quad \text{C-4}$$

$$k = -\frac{1}{0.96(\omega_{st} - 0.2)^{-0.92} + 0.13} \quad \text{C-5}$$

$$\omega_{st} = \frac{2\pi\eta_{rt}\sqrt{\frac{P_{rt}}{\rho}}}{60(gH_{rt})^{\frac{5}{4}}} \quad \text{C-6}$$

$$\frac{P_t}{P_{rt}} = \frac{e^{(0.37\frac{P_t}{P_{nt}} - 1)} - 1}{0.37} + 1 \quad \text{C-7}$$

Due to the complexity involved in these calculations, they are normally done in a computer program.

APPENDIX D: PERFORMANCE FACTOR DIAGRAMS FROM THE METHOD OF CHAPALLAZ ET AL. (1992)

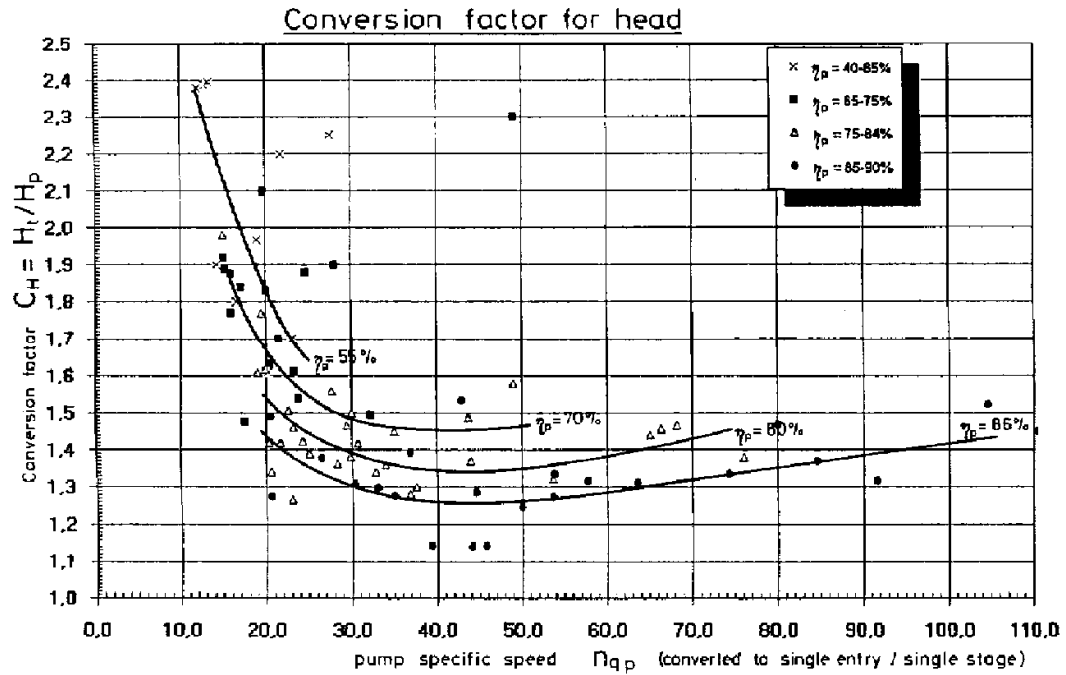


Figure 24: Performance factors, head versus flow

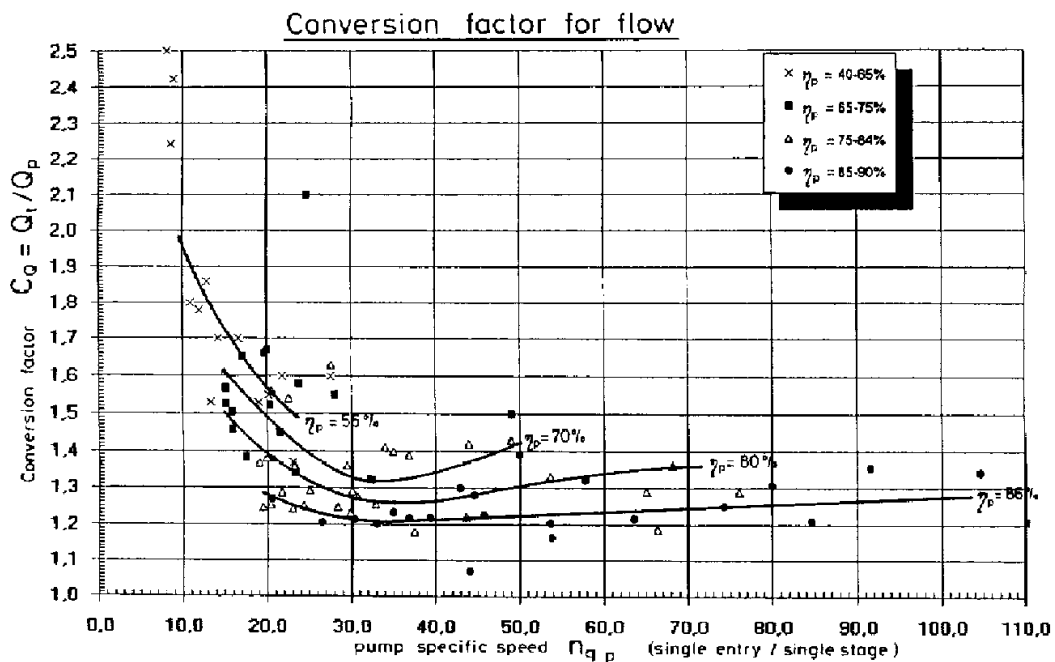


Figure 25: Performance factors, power versus flow

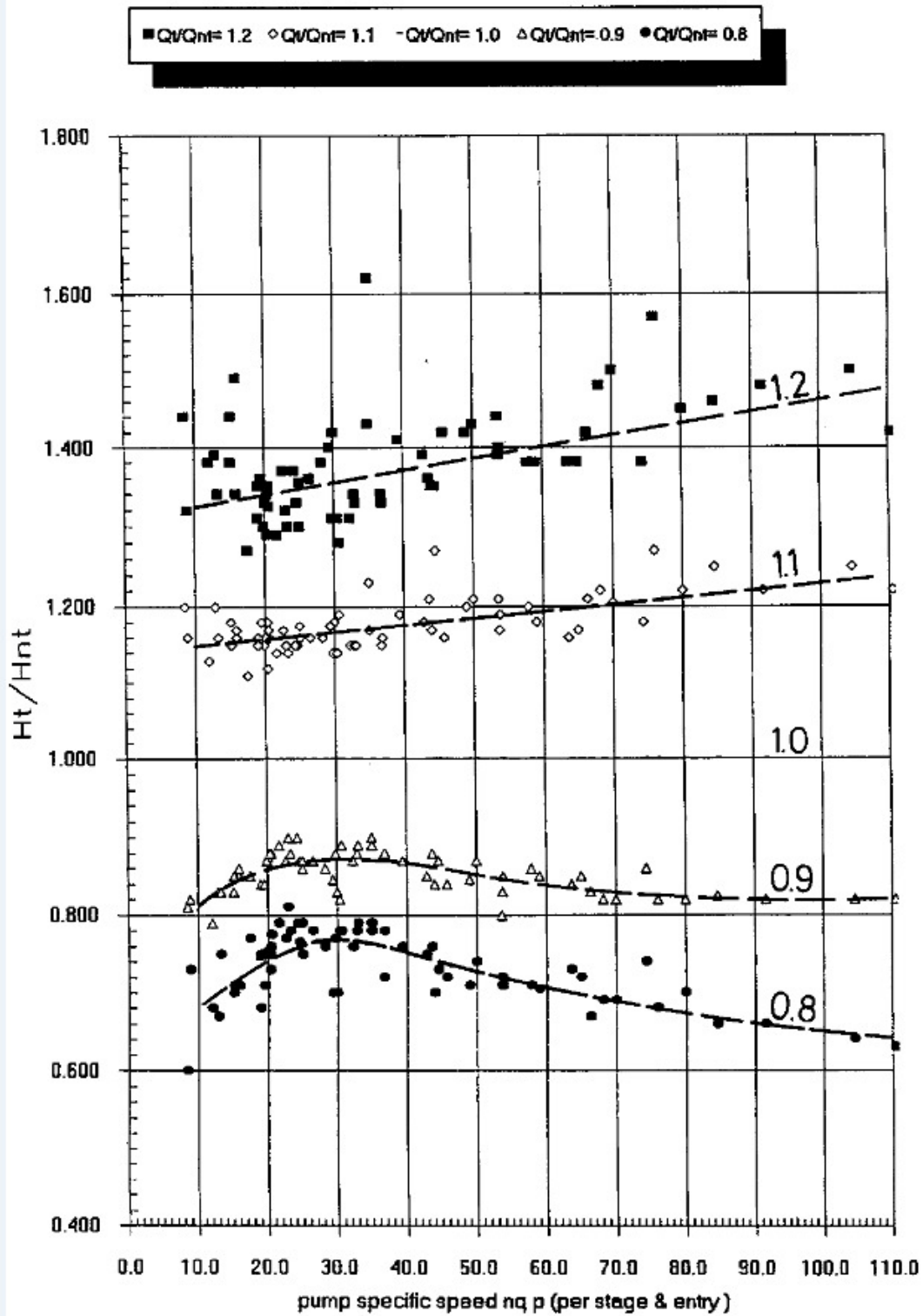


Figure 26: Factors for calculating head away from BEP

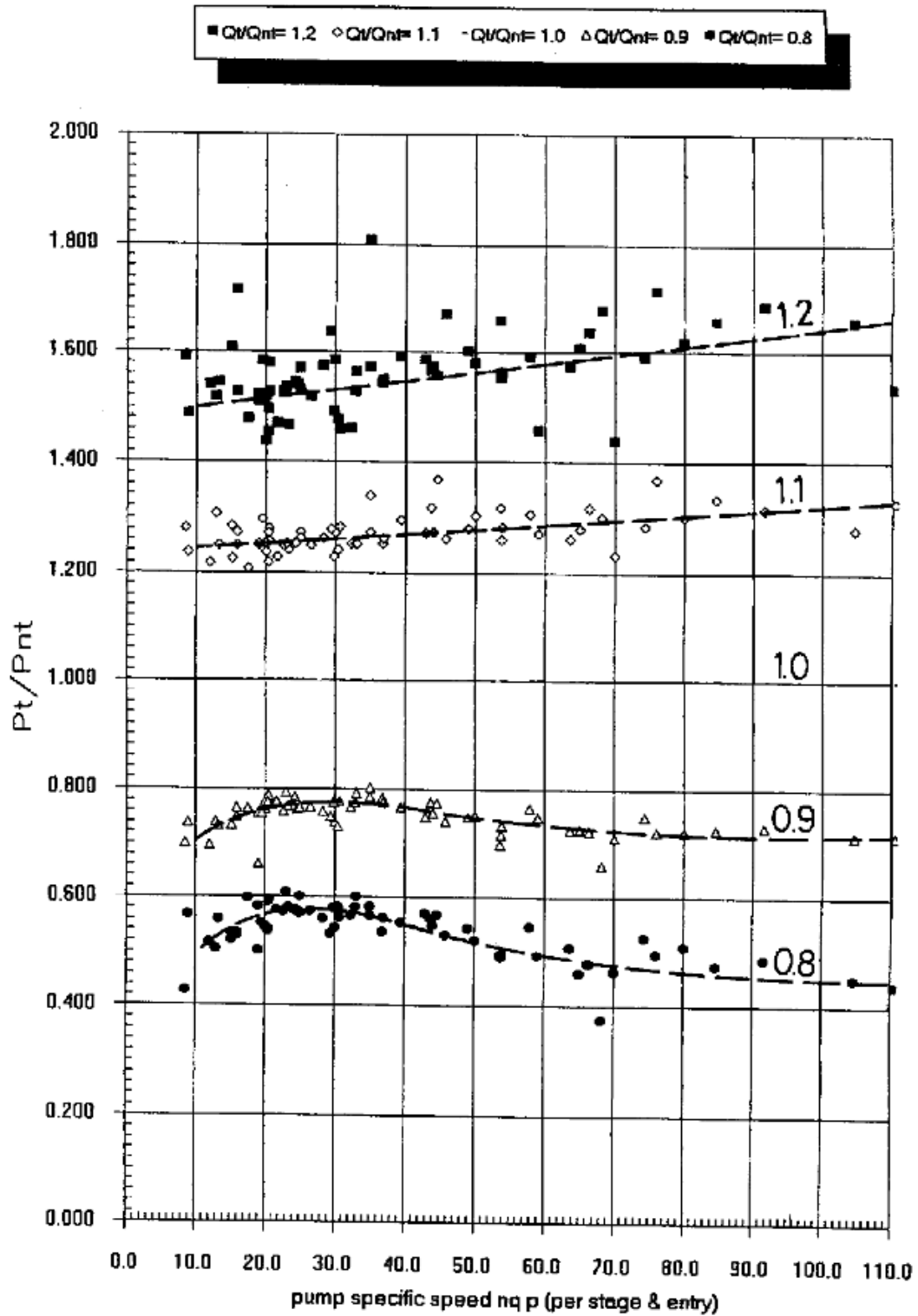


FIGURE 27
 Figure 27: Factors for calculating power away from BEP

APPENDIX F: PUMP AND TURBINE MODE CURVES OF VARIOUS KSB CENTRIFUGAL PUMPS

Baureihe-Größe Type-Size Modèle	Typ Serie Tipo	Nenn Drehzahl Nom. speed Vitesse nom.	Velocità di rotazione nom. Nominal speed Revoluciones nom.	Laufrad-Ø Impeller diameter Diamètre de roue	Ø Garantie Ø Waaler Ø Rodete	
Projekt Project Projet	Progetto Projecto	Angebots-Nr. Project No. No. de l'offre	Offerta-No. Offertnr. Offerta-No.	Pos.-Nr. Item No. No. de pos.	Pos.-Nr. Posiblenr. Pos.-Nr.	
Omega 350-510A Turbine		760 1/min		518 mm		KSB Aldingerwerkstatt 67225 Frankenthal Johann-Joan-Strasse 9 67227 Frankenthal
Roman Bay Sea Farm		2009-09-125				

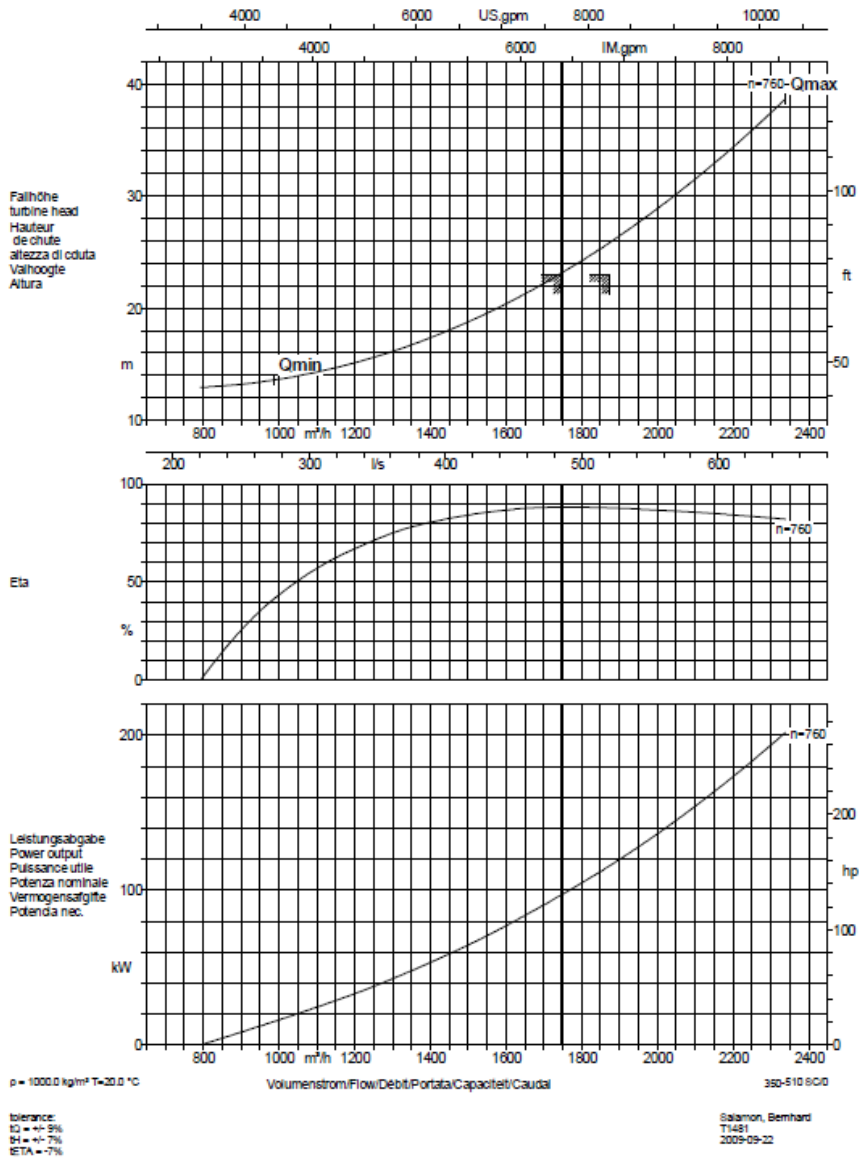


Figure 28: Omega 350-510A in turbine mode

Baureihe-Größe Type-Size Modèle	Typo Serie Tipo	Nenn Drehzahl Nom. speed Vitesse nom.	Velocità di rotazione nom. Nominal foerental Revoluciones nom.	Laufrad-Ø Impeller Dia. Diamètre de roue	Ø Girante Ø Waaler Ø Rodete	
Projekt Project Projet	Progetto Projekt Proyecto	Angebots-Nr. Project No. No. de l'offre	Offerta-No. Offerten- Offerta-No.	Pos.-Nr. Item No. No. de pos.	Pos.-Nr. Positem- Pos.-Nr.	
Omega 350-510A		741 1/min		482 mm		KSB Aktiengesellschaft 67225 Frankfurt Johann-Klein-Straße 9 67227 Frankfurt

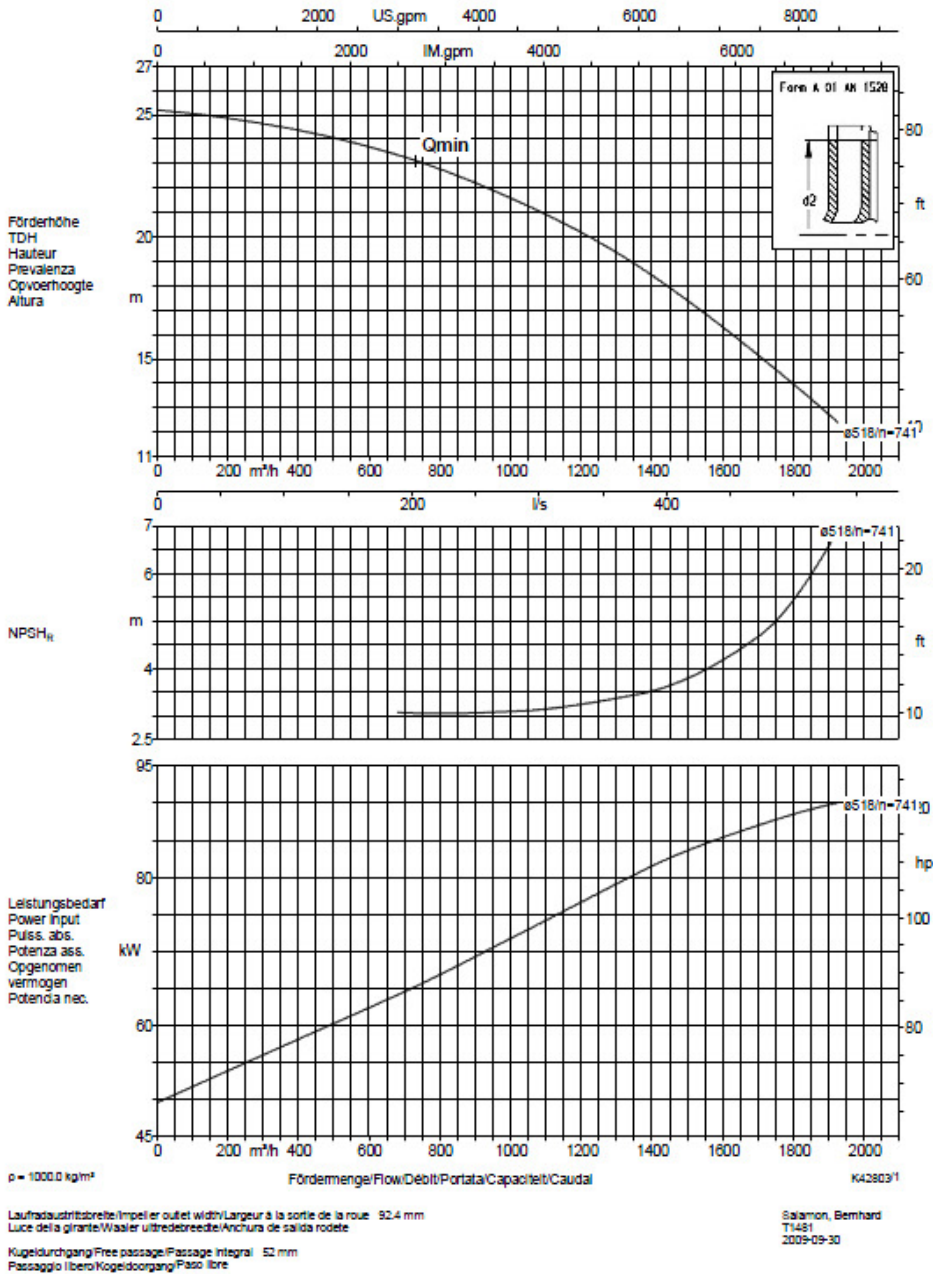


Figure 29: Omega 350-510A in pump mode

Pump Type LCC-M 200-610	Model LCC-M 200-610	Vane Diameter 610mm	Free Passage 102x109mm	 
Clear Water Performance The effects of specific gravity, viscosity and solids on performance with slurry must be accounted for. Alternate choice for frame size or seal type may also have some effects.	Frame Size 3	Seal Type P, M	Curve Number E 12G-87 Test B305B-93	

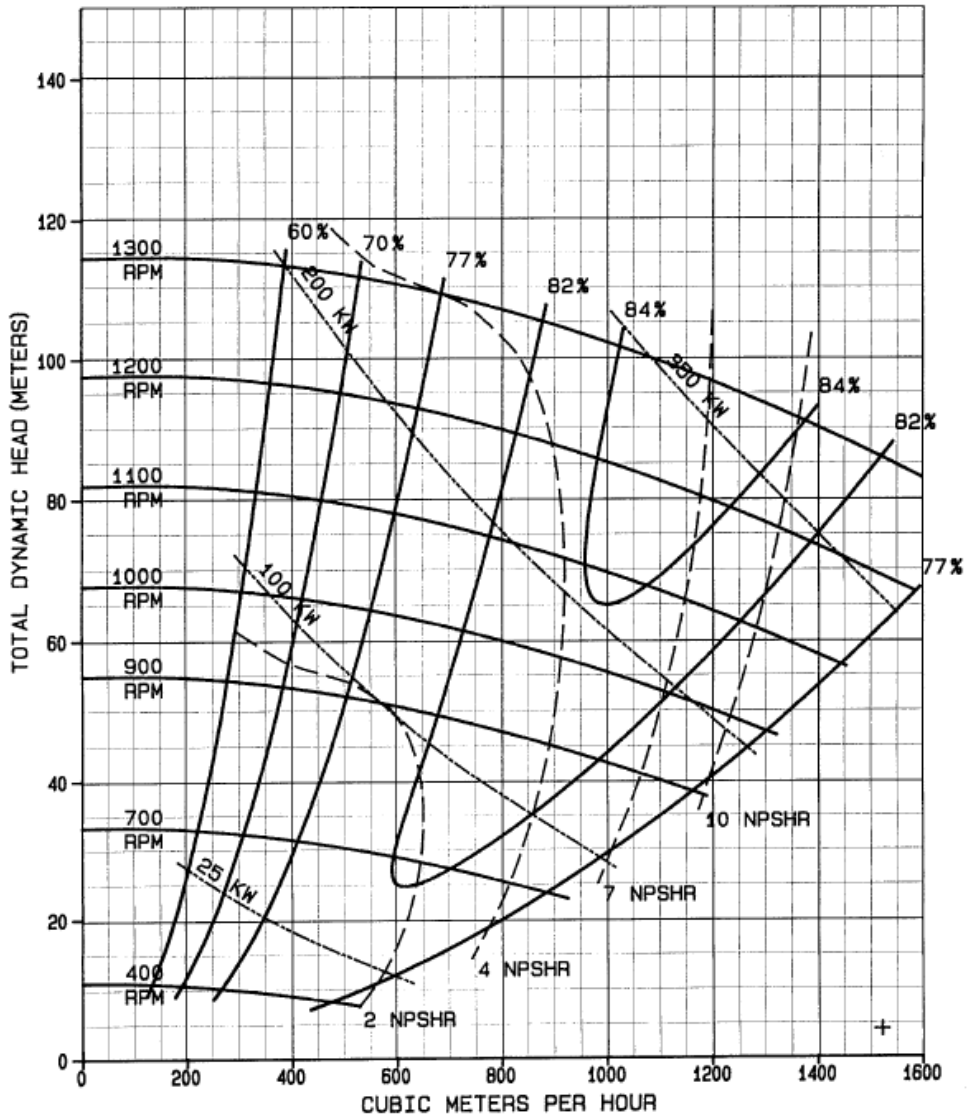


Figure 30: Pump curve of KSB LCC-M 200-610 pump